

AWARD NUMBER: W81XWH-17-1-0129

TITLE: Targeting the Cell Surfaceome of Aggressive Neuroendocrine Prostate Cancer

PRINCIPAL INVESTIGATOR: John K. Lee, M.D., Ph.D.

CONTRACTING ORGANIZATION: University of California, Los Angeles
Los Angeles, CA 90095

REPORT DATE: July 2018

TYPE OF REPORT: Annual

PREPARED FOR: U.S. Army Medical Research and Materiel Command
Fort Detrick, Maryland 21702-5012

DISTRIBUTION STATEMENT: Approved for Public Release; Distribution Unlimited

The views, opinions and/or findings contained in this report are those of the author(s) and should not be construed as an official Department of the Army position, policy or decision unless so designated by other documentation.

REPORT DOCUMENTATION PAGE

Form Approved
OMB No. 0704-0188

Public reporting burden for this collection of information is estimated to average 1 hour per response, including the time for reviewing instructions, searching existing data sources, gathering and maintaining the data needed, and completing and reviewing this collection of information. Send comments regarding this burden estimate or any other aspect of this collection of information, including suggestions for reducing this burden to Department of Defense, Washington Headquarters Services, Directorate for Information Operations and Reports (0704-0188), 1215 Jefferson Davis Highway, Suite 1204, Arlington, VA 22202-4302. Respondents should be aware that notwithstanding any other provision of law, no person shall be subject to any penalty for failing to comply with a collection of information if it does not display a currently valid OMB control number. **PLEASE DO NOT RETURN YOUR FORM TO THE ABOVE ADDRESS.**

1. REPORT DATE July 2018			2. REPORT TYPE Annual		3. DATES COVERED 07/01/2017 - 06/30/18	
4. TITLE AND SUBTITLE Targeting the Cell Surfaceome of Aggressive Neuroendocrine Prostate Cancer					5a. CONTRACT NUMBER	
					5b. GRANT NUMBER W81XWH-17-1-0129	
					5c. PROGRAM ELEMENT NUMBER	
6. AUTHOR(S) John K. Lee, M.D., Ph.D. E-Mail: jklee5@fredhutch.org					5d. PROJECT NUMBER	
					5e. TASK NUMBER	
					5f. WORK UNIT NUMBER	
7. PERFORMING ORGANIZATION NAME(S) AND ADDRESS(ES) University of California, Los Angeles 10889 Wilshire Blvd. Ste. 700 Los Angeles, CA 90095-0001					8. PERFORMING ORGANIZATION REPORT NUMBER	
9. SPONSORING / MONITORING AGENCY NAME(S) AND ADDRESS(ES) U.S. Army Medical Research and Materiel Command Fort Detrick, Maryland 21702-5012					10. SPONSOR/MONITOR'S ACRONYM(S)	
					11. SPONSOR/MONITOR'S REPORT NUMBER(S)	
12. DISTRIBUTION / AVAILABILITY STATEMENT Approved for Public Release; Distribution Unlimited						
13. SUPPLEMENTARY NOTES						
14. ABSTRACT In this reporting period, we have performed transcriptomic and cell surface proteomic profiling of a panel of human prostate cancer cell lines and integrated these data sets to nominate high-confidence cell surface antigens associated with neuroendocrine prostate cancer (NEPC) and prostate adenocarcinoma (PrAd). Validation of candidate antigens is ongoing but several have demonstrated prostate cancer subtype-specific protein expression based on immunoblotting, immunohistochemistry, and flow cytometry of prostate cancer cell lines, xenografts, and clinical prostate cancer tissues. For example, we have characterized CEACAM5 (carcinoembryonic antigen 5) as a cell surface marker expressed in 60% of NEPC but not in PrAd. This finding has led to new projects in the laboratory with potential for clinical translation related to therapeutically targeting CEACAM5-positive NEPC with an antibody-drug conjugate or chimeric antigen receptor T cell immunotherapy.						
15. SUBJECT TERMS Neuroendocrine prostate cancer, cell surface antigens, antibody therapy, immunotherapy						
16. SECURITY CLASSIFICATION OF:			17. LIMITATION OF ABSTRACT Unclassified	18. NUMBER OF PAGES 32	19a. NAME OF RESPONSIBLE PERSON USAMRMC	
a. REPORT Unclassified	b. ABSTRACT Unclassified	c. THIS PAGE Unclassified			19b. TELEPHONE NUMBER (include area code)	

Table of Contents

	<u>Page</u>
1. Introduction	1
2. Keywords	1
3. Accomplishments	1
4. Impact	4
5. Changes/Problems	4
6. Products	4
7. Participants & Other Collaborating Organizations	5
8. Special Reporting Requirements	5
9. References	6
10. Appendix	7

INTRODUCTION

Background: Neuroendocrine prostate cancer (NEPC) is a common, deadly endpoint for men with late-stage metastatic prostate cancer. Up to 20% of men with lethal metastatic prostate cancer have demonstrated evidence of NEPC [1, 2]. NEPC can be distinguished from conventional prostate cancer or prostate adenocarcinoma (PrAd) by histologic features, neuroendocrine marker expression, loss of either androgen receptor (AR) or downstream AR signaling, Polycomb repressive complex expression, and global methylation patterns [3-5]. NEPC apparently represents a cancer differentiation state distinct from PrAd and we hypothesize that the cell surface phenotype of these prostate cancer subtypes should reflect these differences. Furthermore, these differences in cell surface antigen expression may provide an opportunity for prostate cancer subtype-specific therapeutic targeting. The purpose of the research is to establish new NEPC models, to characterize the differential cell surface antigen profile of NEPC relative to PrAd, and to develop new antibody reagents targeting novel antigens in NEPC. We believe that these studies may facilitate the development of targeted treatments for men with NEPC, for which there are no currently available FDA-approved therapeutics.

KEYWORDS

Neuroendocrine prostate cancer, cell surface antigens, antibody therapy, immunotherapy

ACCOMPLISHMENTS

To summarize the research accomplishments to date, the tasks described in the proposed Statement of Work are itemized here with a brief update for each task.

SA 1: *Establish a diverse panel of NEPC cell lines from human prostate epithelial transformation (months 1-12)*

Task 1: Use the human prostate organoid transformation assay with the oncogenes MYCN and activated AKT1 to generate new NEPC cell lines (months 1-12) Completed.

We have generated five NEPC cell lines using the human prostate transformation assay called LASCPC-01, NA1, NA2, NA3, and NA4. Characterization of these cell lines and xenografts have been performed at the level of morphology, xenograft histology, and transcriptome analysis. LASCPC-01 has been submitted to the ATCC biorepository and is currently available (ATCC CRL-3356) to the research community.

Task 2: Evaluate the effect of p53 loss and Rb loss in combination with the oncogenes MYCN and activated AKT1 in initiation of NEPC (months 1-24) Not yet started. However, colleagues and I have evaluated the combination of c-Myc, activated AKT1, p53 (R175H), and shRb in the human prostate epithelial transformation assay. This combination of oncogenic insults produces a highly penetrant small cell NEPC phenotype, from which three cell lines have been developed and characterized. A manuscript describing these results is being prepared. We anticipate that substitution of c-Myc with N-Myc in this gene combination should also generate a small cell NEPC phenotype.

SA 2: *Validate candidate cell surface markers on NEPC using proteomic approaches*

Task 1: High-throughput cell surface proteomic analysis of prostate cancer cell lines (months 1-14) Completed. We have evaluated a panel of prostate cancer cell lines by cell

surface biotinylation, streptavidin affinity purification, and liquid chromatography/mass spectrometry to quantitate cell surface protein expression in collaboration with Dr. James Wohlschlegel at UCLA. The results of these experiments have been reported in our publication in *The Proceedings of the National Academy of Sciences* (Appendix 1). We identified 1080 total proteins from these studies, of which 45.6% were annotated by Gene Ontology as “plasma membrane” in localization (Appendix 1, Fig. 3A). We also integrated the cell surface proteomics data with RNA-Seq gene expression data, focusing on genes putatively encoding cell surface proteins (“cell surface genes”), by a technique called rank-rank hypergeometric overlap (RRHO) [6]. We used RRHO to examine the NEPC and PrAd subsets and plot differentially enriched cell surface genes from the transcriptome data vs. differentially enriched cell surface proteins from the proteome data. We focused on genes/proteins enriched in NEPC by both the transcriptomic and proteomic data as being high-confidence cell surface candidates in NEPC (Appendix 1, Fig. 3C).

Task 2: Validation of candidate cell surface proteins using low-throughput proteomic techniques (months 6-18) In progress. We are currently performing multi-level validation of candidate NEPC cell surface marker expression by immunoblotting, immunohistochemistry, and flow sorting of NEPC cell lines, xenografts, and archived tumors. The rigor employed in validating nominated cell surface antigens is evident in the example of CEACAM5 (Appendix 1, Fig. 4 and Fig. 6), an antigen whose prostate cancer subtype-specific expression in NEPC was uncovered through our analysis. CEACAM5 is expressed at moderate-to-strong levels in approximately 60% of NEPC tumors analyzed.

Task 3: Prioritization of candidate NEPC cell surface proteins for therapeutic development (months 6-18) In progress. Our approach to the prioritization of candidate antigens involves the scope of systemic expression in normal tissues. We are performing analysis of the NIH GTEx database to evaluate RNA-level expression as well as immunoblot and immunohistochemistry to determine protein-level expression of candidate antigens in normal human tissues. Our initial studies indicate that the candidate prostate cancer antigens identified are not exclusively cancer-specific and are often expressed at varying levels in normal human tissues as well (Appendix 1, Fig. S5 and Fig. S8). We have taken the approach of prioritizing those with the fewest tissues in which expression is seen and with the lowest levels of gene/protein expression. However, prior experience with antibody and antibody-drug conjugate therapies have suggested that the dose-limiting toxicities of these agents do not correlate well with the systemic expression of their targets.

SA 3: Develop novel antibody reagents targeting cell surface antigens in NEPC (months 18-48)

Task 1: Human scFv phage display library screening to identify antibody reagents (months 18-32) Not yet started.

Task 2: Validation of the specificity and performance of human monoclonal antibodies derived from phage display screening (months 18-34) Not yet started.

Task 3: Therapeutic evaluation of monoclonal antibodies against candidate cell surface targets (months 30-40) Not yet started.

Task 4: Mouse studies with therapeutic monoclonal antibodies in NEPC (months 40-48) Not yet started.

Key Research Accomplishments:

- We have developed multiple human NEPC cell lines based on the transformation of human prostate epithelial cells with N-Myc and activated AKT1.
- We have shown, from gene expression analyses focused on a bioinformatically derived set of genes that are predicted to encode plasma membrane proteins, that NEPC and PrAd samples can be readily discriminated based on cell surface phenotypes.
- Multiple putative NEPC cell surface antigens have been identified through the integration of transcriptome and cell surface proteome data from a panel of human prostate cancer cell lines. A prime example is CEACAM5 which has not previously been described as a significant prostate cancer antigen. These results and the proof-of-concept of targeting CEACAM5 in NEPC with chimeric antigen receptor (CAR) T cell immunotherapy have recently been published.

Opportunities for Training and Professional Development:

During this reporting period, opportunities for training included attendance at the Proteomics Seminar Series at UCLA as well as completion of the UCLA Institute for Quantitative and Computational Biosciences Collaboratory Workshops. These programs provided training in understanding approaches to quantitative proteomic analysis, the analysis of RNA-Seq data from raw reads, and the integration of large datasets. Professional development of leadership has been critical in my role as co-leader of the Prostate Cancer Foundation Young Investigator Tumorigenesis Working Group. In addition, establishing and guiding a new laboratory at the Fred Hutch as a principal investigator has provided and will continue to generate many learning experiences related to leadership. At Fred Hutch, I am actively establishing a junior faculty mentoring committee at Fred Hutch that includes Dr. Pete Nelson who is a pre-eminent figure in the field of prostate cancer. In addition, I have developed mentoring networks through my involvement with the Prostate Cancer Foundation, UCLA SPORE in Prostate Cancer, and the Pacific Northwest Prostate Cancer SPORE.

Dissemination of Results:

Results of these studies have been disseminated to the prostate cancer research community through a poster presentation at the Prostate Cancer Foundation Annual Scientific Meeting from October 5-7, 2017 and by our recent publication in *The Proceedings of the National Academy of Sciences* (Appendix 1).

Plan for the Next Reporting Period:

In the next reporting period, we will initiate human prostate organoid transformation studies evaluating the effect of p53 loss and Rb loss in combination with the oncogenes MYCN and activated AKT1 in initiation of NEPC from Specific Aim 1, Task 2. We will also continue low-throughput proteomic validation studies and prioritization of candidate NEPC cell surface antigens by evaluating the scope and intensity of expression in normal human tissues. Extracellular domains of fully validated antigens will then be submitted for phage display

antibody screening to identify antibody reagents which will be vetted for their specificity and affinity as outlined in Specific Aim 3, Tasks 1-2.

IMPACT

The specific discovery and validation of CEACAM5 expression in over 60% of NEPC samples has prompted pre-clinical investigation into whether targeting CEACAM5 in NEPC may be a viable treatment strategy. We have provided evidence that CEACAM5 CAR T cell immunotherapy can be engineered and optimized to promote antigen-specific NEPC killing *in vitro* (Appendix 1, Fig. 7). These preliminary studies have formed the basis for a team science Prostate Cancer Foundation Challenge Award (PI's: Owen Witte, John Lee, Stephen Forman, Saul Priceman) to investigate the safety and efficacy of CEACAM5 CAR T cell immunotherapy for NEPC in clinically relevant, immune-competent mouse models.

CEACAM5-directed therapies are in active development for colorectal cancer. Specifically, antibody-drug conjugates (ADCs) targeting CEACAM5 have shown efficacy and a manageable toxicity profile in a phase I/II clinical trial of heavily pretreated patients with metastatic colorectal cancer [7]. We are planning to evaluate a CEACAM5 ADC in patient-derived xenograft models of NEPC with the idea that these studies may establish the scientific framework for a potential clinical trial of CEACAM5 ADC therapy in CEACAM5-positive NEPC.

CHANGES/PROBLEMS

The project has been somewhat impacted by my relocation from UCLA to Fred Hutchinson Cancer Research Center because of a temporary loss of productivity related to establishing a new laboratory and resuming research efforts. However, I do not believe that this will hamper our ability to achieve the milestones proposed. The project and its direction are otherwise unchanged.

PRODUCTS

Publication: Lee JK, Bangayan NJ, Chai T, Smith BA, Pariva TE, Yun S, Vashisht A, Zhang Q, Park JW, Corey E, Huang J, Graeber TG, Wohlschlegel J, Witte ON. *Systemic surfaceome profiling identifies target antigens for immune-based therapy in subtypes of advanced prostate cancer*. Proc Natl Acad Sci U S A, 2018. April 23. [Epub ahead of print]

PARTICIPANTS & OTHER COLLABORATING ORGANIZATIONS

Name:	<i>John K. Lee</i>
Project Role:	<i>PI</i>
Researcher Identifier (e.g. ORCID ID):	https://orcid.org/0000-0002-6570-2180
Nearest person month worked:	<i>3</i>
Contribution to Project:	<i>Dr. Lee has performed data analysis and overseen the conduct of the study.</i>
Funding Support:	

Name:	<i>Tiffany Pariva</i>
Project Role:	<i>Research Technician</i>
Researcher Identifier (e.g. ORCID ID):	
Nearest person month worked:	<i>5</i>
Contribution to Project:	<i>Ms. Pariva has performed low-throughput proteomic analyses to validate the expression of candidate prostate cancer subtype-specific antigens in cell lines, xenografts, and archived clinical tissues.</i>
Funding Support:	

SPECIAL REPORTING REQUIREMENTS

Nothing to Report.

REFERENCES

1. Tanaka, M., et al., *Progression of prostate cancer to neuroendocrine cell tumor*. Int J Urol, 2001. **8**(8): p. 431-6; discussion 437.
2. Bluemn, E.G., et al., *Androgen Receptor Pathway-Independent Prostate Cancer Is Sustained through FGF Signaling*. Cancer Cell, 2017. **32**(4): p. 474-489.e6.
3. Yao, J.L., et al., *Small cell carcinoma of the prostate: an immunohistochemical study*. Am J Surg Pathol, 2006. **30**(6): p. 705-12.
4. Clermont, P.L., et al., *Polycomb-mediated silencing in neuroendocrine prostate cancer*. Clin Epigenetics, 2015. **7**: p. 40.
5. Beltran, H., et al., *Divergent clonal evolution of castration-resistant neuroendocrine prostate cancer*. Nat Med, 2016. **22**(3): p. 298-305.
6. Plaisier, S.B., et al., *Rank-rank hypergeometric overlap: identification of statistically significant overlap between gene-expression signatures*. Nucleic Acids Res, 2010. **38**(17): p. e169.
7. Dotan, E., et al., *Phase I/II Trial of Labetuzumab Govitecan (Anti-CEACAM5/SN-38 Antibody-Drug Conjugate) in Patients With Refractory or Relapsing Metastatic Colorectal Cancer*. J Clin Oncol, 2017. **35**(29): p. 3338-3346.

APPENDICES

- Appendix 1: Lee JK, Bangayan NJ, Chai T, Smith BA, Pariva TE, Yun S, Vashisht A, Zhang Q, Park JW, Corey E, Huang J, Graeber TG, Wohlschlegel J, Witte ON. *Systemic surfaceome profiling identifies target antigens for immune-based therapy in subtypes of advanced prostate cancer*. Proc Natl Acad Sci U S A, 2018. April 23. [Epub ahead of print]



Systemic surfaceome profiling identifies target antigens for immune-based therapy in subtypes of advanced prostate cancer

John K. Lee^{a,b,c}, Nathanael J. Bangayan^d, Timothy Chai^e, Bryan A. Smith^f, Tiffany E. Pariva^f, Sangwon Yun^g, Ajay Vashisht^h, Qingfu Zhang^{ij}, Jung Wook Park^f, Eva Corey^k, Jiaoti Huang^j, Thomas G. Graeber^{c,d,l,m}, James Wohlschlegel^h, and Owen N. Witte^{c,d,f,n,o,1}

^aDivision of Hematology and Oncology, Department of Medicine, University of California, Los Angeles, CA 90095; ^bInstitute of Urologic Oncology, Department of Urology, University of California, Los Angeles, CA 90095; ^cJonsson Comprehensive Cancer Center, University of California, Los Angeles, CA 90095; ^dDepartment of Molecular and Medical Pharmacology, University of California, Los Angeles, CA 90095; ^eStanford University School of Medicine, Palo Alto, CA 94305; ^fDepartment of Microbiology, Immunology, and Medical Genetics, University of California, Los Angeles, CA 90095; ^gYale School of Medicine, New Haven, CT 06510; ^hDepartment of Biological Chemistry, University of California, Los Angeles, CA 90095; ⁱDepartment of Pathology, Duke University School of Medicine, Durham, NC 27708; ^jDepartment of Pathology, China Medical University, 110001 Shenyang, People's Republic of China; ^kDepartment of Urology, University of Washington School of Medicine, Seattle, WA 98195; ^lCrump Institute for Molecular Imaging, University of California, Los Angeles, CA 90095; ^mUCLA Metabolomics Center, University of California, Los Angeles, CA 90095; ⁿParker Institute for Cancer Immunotherapy, University of California, Los Angeles, CA 90095; and ^oEli and Edythe Broad Center of Regenerative Medicine and Stem Cell Research, University of California, Los Angeles, CA 90095

Contributed by Owen N. Witte, March 28, 2018 (sent for review February 8, 2018; reviewed by Massimo Loda and Cassian Yee)

Prostate cancer is a heterogeneous disease composed of divergent molecular and histologic subtypes, including prostate adenocarcinoma (PrAd) and neuroendocrine prostate cancer (NEPC). While PrAd is the major histology in prostate cancer, NEPC can evolve from PrAd as a mechanism of treatment resistance that involves a transition from an epithelial to a neurosecretory cancer phenotype. Cell surface markers are often associated with specific cell lineages and differentiation states in normal development and cancer. Here, we show that PrAd and NEPC can be broadly discriminated by cell-surface profiles based on the analysis of prostate cancer gene expression datasets. To overcome a dependence on predictions of human cell-surface genes and an assumed correlation between mRNA levels and protein expression, we integrated transcriptomic and cell-surface proteomic data generated from a panel of prostate cancer cell lines to nominate cell-surface markers associated with these cancer subtypes. FXYD3 and CEACAM5 were validated as cell-surface antigens enriched in PrAd and NEPC, respectively. Given the lack of effective treatments for NEPC, CEACAM5 appeared to be a promising target for cell-based immunotherapy. As a proof of concept, engineered chimeric antigen receptor T cells targeting CEACAM5 induced antigen-specific cytotoxicity in NEPC cell lines. Our findings demonstrate that the surfaceomes of PrAd and NEPC reflect unique cancer differentiation states and broadly represent vulnerabilities amenable to therapeutic targeting.

prostate cancer | cell surface antigens | immunotherapy

Prostate cancer is the most common non-skin cancer diagnosed in men and the second leading cause of cancer death in men (1). More than 95% of prostate cancers are diagnosed as prostate adenocarcinoma (PrAd), which is characterized by glandular epithelial architecture, expression of luminal cytokeratins (CK8 and CK18), and active androgen receptor (AR) signaling. In advanced disease, blockade of AR signaling has been the mainstay of treatment for decades, but inevitably leads to resistance in the form of castration-resistant prostate cancer (CRPC). Recent data indicate that CRPC can retain the PrAd histology or recur as a distinct subtype called neuroendocrine prostate cancer (NEPC). Recent work also indicates that a subset of CRPC assumes a double-negative (AR- and neuroendocrine-negative) phenotype that is maintained by enhanced FGF and MAPK pathway signaling (2). NEPC describes a group of neuroendocrine tumors that includes aggressive variants such as large- and small-cell carcinoma of the prostate (3). Aggressive, treatment-related NEPC evolves from PrAd in up to 20% of CRPC cases through neuroendocrine trans-

differentiation, which involves epigenetic reprogramming mediated by Polycomb proteins (4, 5) and often the loss of the tumor suppressors RB1 and TP53 (6). NEPC often exhibits an anaplastic morphology, expression of neuroendocrine markers including chromogranins and synaptophysin, loss of AR signaling, overexpression and amplification of MYCN and AURKA (7–9), and a particularly poor prognosis due to rapid and progressive metastatic dissemination.

Treatments for CRPC have expanded in recent years to include second-generation antiandrogen therapies, vaccine immunotherapy, an alpha particle-emitting radioactive agent, and additional cytotoxic chemotherapy (10). Notably, the characterization of prostate cancer cell-surface antigens like prostate-specific membrane antigen (PSMA) has spurred the development of novel diagnostic imaging and targeted therapeutic strategies. For example, PSMA-based positron emission tomography has demonstrated

Significance

Advanced prostate cancer is a deadly disease made up of multiple cancer subtypes that evolve during its natural history. Unfortunately, antibody- and cell-based therapies in development that target single tumor antigens found in conventional prostate cancer do not account for this heterogeneity. Here, we show that two major subtypes of advanced prostate cancer, prostate adenocarcinoma (PrAd) and neuroendocrine prostate cancer (NEPC), exhibit distinct cell-surface expression profiles. Integrated analysis of gene expression and cell-surface protein expression of prostate cancer nominated multiple subtype-specific cell-surface antigens. We specifically characterize FXYD3 and CEACAM5 as targets for immune-based therapies in PrAd and NEPC and provide preliminary evidence of the antigen-specific cytotoxic activity of CEACAM5-directed chimeric antigen receptor T cells in NEPC.

Author contributions: J.K.L. and O.N.W. designed research; J.K.L., N.J.B., T.C., T.E.P., S.Y., and A.V. performed research; J.K.L., N.J.B., T.C., B.A.S., and E.C. contributed new reagents/analytic tools; J.K.L., N.J.B., T.C., B.A.S., T.E.P., S.Y., A.V., Q.Z., J.W.P., E.C., J.H., T.G.G., and J.W. analyzed data; and J.K.L. and O.N.W. wrote the paper.

Reviewers: M.L., Dana Farber Cancer Institute; and C.Y., MD Anderson Cancer Center.

The authors declare no conflict of interest.

This open access article is distributed under [Creative Commons Attribution-NonCommercial-NoDerivatives License 4.0 \(CC BY-NC-ND\)](https://creativecommons.org/licenses/by-nc-nd/4.0/).

¹To whom correspondence should be addressed. Email: owenwitte@mednet.ucla.edu.

This article contains supporting information online at www.pnas.org/lookup/suppl/doi:10.1073/pnas.1802354115/-DCSupplemental.

To determine whether the cell-surface phenotype was more highly conserved in PrAd or NEPC, we used rank–rank hypergeometric overlap (RRHO) analysis (25) to compare the ranked differential expression of genes encoding cell-surface proteins (heretofore called “cell surface genes”) between prostate cancer subtypes in multiple datasets [WCDT from the Stand Up To Cancer/American Association for Cancer Research/Prostate Cancer Foundation West Coast Dream Team (26), Beltran 2016 (14), and Zhang 2015 (24)]. This rank-based methodology circumvents the complications of normalization for specific sample preparations and analysis platforms, enabling facile comparisons of gene expression across defined classes of prostate cancer in published datasets. Pairwise evaluation of the datasets revealed higher rank correlation of cell-surface genes enriched in NEPC (Fig. 1C), supporting stronger homogeneity of cell-surface phenotypes in NEPC than in PrAd.

Differential expression analysis of the Beltran 2016 dataset showed that the expression of 330 cell-surface genes was enriched fourfold or more in the PrAd samples, while expression of 438 cell-surface genes was similarly enriched in the NEPC samples. PANTHER (Protein ANnotation THrough Evolutionary Relationship) analysis was performed to compare differentially expressed genes to a reference gene list to identify enriched molecular functions and biological processes (27). PANTHER overrepresentation testing of the cell-surface genes enriched in NEPC in the Beltran 2016 dataset identified gene ontologies related to neural functions, including synaptic signaling, nervous system development, and neurotransmitter transport (Fig. 1D). In contrast, analysis of cell-surface genes enriched in PrAd from the same dataset revealed biological processes involving secretion, immune response, and inflammatory response (Fig. 1E). The results highlight substantial differences in cell-surface antigen expression linked to the cancer differentiation states of NEPC and PrAd.

Identification of Candidate Prostate Cancer Cell-Surface Antigens by Transcriptomic Analysis. We next assembled a diverse panel of human prostate cancer cell lines to further characterize cell-surface antigens in the PrAd and NEPC subtypes. The panel included established lines including CWR22Rv1, LNCaP, NE1.3 (28), DU145, NCI-H660, and LASCPC-01 (8), as well as two developed cell lines named NB120914 and MSKCC EF1. NB120914 was initiated from an intraoperative biopsy of a metastatic castration-resistant PrAd involving the femur. While the original tumor showed a luminal phenotype with CK8 and AR expression, the resultant PDX tumor and subsequent cell-line xenograft tumors lacked expression of both luminal and neuroendocrine markers, indicative of the development of double-negative (AR- and neuroendocrine-negative) prostate cancer (*SI Appendix, Fig. S2 A, B, and D*) (2). MSKCC EF1 was adapted from 3D organoid culture (29) to suspension culture and formed xenograft tumors marked by NEPC histology, absence of AR, and expression of the neuroendocrine marker synaptophysin and p63 (*SI Appendix, Fig. S2 C and E*).

RNA-seq gene-expression analysis revealed significant heterogeneity in expression of androgen-regulated genes, neuroendocrine markers, and epithelial markers in the cell line panel (Fig. 2A), demonstrating a diverse range of molecular phenotypes. Unsupervised hierarchical clustering analysis of the prostate cancer cell lines based on the expression of cell-surface genes yielded clusters of NEPC lines (MSKCC EF1 and NCI-H660), AR-negative PrAd lines (DU145 and LASCPC-01 marked by mixed NEPC and PrAd phenotypes and NB120914), and AR-positive PrAd lines (CWR22Rv1, LNCaP, and the LNCaP-derivative NE1.3) (Fig. 2B). Differential cell-surface gene expression was evaluated in the PrAd and NEPC cell lines and identified the established PrAd markers PSCA and FOLH1 (PSMA), as well as the NEPC marker neural cell adhesion molecule 1 (NCAM1) (Fig. 2C).

We then integrated multiple prostate cancer gene expression datasets to identify differentially expressed PrAd- and NEPC-specific cell-surface markers that are conserved in prostate cancer

cell lines, PDXs, and patient tumors. For each of the datasets (WCDT, Beltran 2016, Zhang 2015 LuCaP PDXs, Zhang 2015 metastatic CRPC, and prostate cancer cell line panel), we performed rank overlap analysis by ranking the top 500 differentially expressed PrAd or NEPC cell-surface genes from each dataset and evaluating the overlap of these genes across datasets. A total of 21 genes were enriched in PrAd samples in all datasets, including well-established biomarkers and target antigens for prostate cancer therapeutics such as FOLH1 (PSMA), TACSTD2 (Trop2), and STEAP1 (Fig. 2D and [Dataset S2](#)). A total of 56 genes were commonly identified in NEPC samples across the datasets ([Dataset S2](#)). Notable from this set of genes were RET, DLL3, and SEZ6 that have been identified as disease markers in neuroendocrine cancers, including medullary thyroid cancer, small- and large-cell lung cancer, and malignant pheochromocytoma (30–32).

Prioritization of High-Confidence Cell-Surface Markers by Integrated Proteomic and Transcriptomic Analysis. While transcriptomic analysis of the prostate cancer subsets for the identification of cell-surface antigens appeared informative, we needed to overcome (i) any inaccuracy of bioinformatic predictions of human cell-surface genes and (ii) the potential for discordance between mRNA levels and protein expression (33). We therefore directly profiled the surfaceomes of the prostate cancer cell-line panel by incubation with a membrane-impermeable biotin to label primary amines on extracellular domains of cell-surface proteins, cell lysis, streptavidin-affinity purification to enrich for biotinylated proteins, trypsin digestion, and quantitative proteomic mass spectrometry (34, 35). Then, 1,080 total proteins were identified, with 45.6% annotated for plasma membrane localization by Gene Ontology (Fig. 3A). Unsupervised clustering of the cell lines based on cell-surface proteomics showed two major clusters with NEPC and AR-negative PrAd lines segregated from AR-positive PrAd lines (Fig. 3A). To evaluate the relative concordance of the cell-surface gene expression and proteomic data from the cell lines, we compared the expression levels of known prostate cancer surface markers including FOLH1 (PSMA), STEAP1, and NCAM1. The gene- and protein-level expression of these markers in the cell-line panel were similar (Fig. 3B), with minor exceptions likely explained by protein-specific availability of primary amines for biotinylation, limitations in the sensitivity of mass spectrometry, and inherent variation in the abundance of proteins and their cognate mRNAs.

As a strategy to identify high-confidence markers in the NEPC and PrAd lines, we integrated the transcriptomic and proteomic data by RRHO analysis to prioritize surface markers that are enriched at the mRNA level and exhibit differential protein expression. Overall, the rank correlation between differentially expressed cell-surface genes and proteins was highest in the NEPC lines (Fig. 3C). We generated a composite rank by arbitrarily assigning equal weights to the proteomics and transcriptomics ranks of differentially expressed proteins or genes for each prostate cancer subset (Fig. 3D). Of the candidates with high composite ranks, the PrAd-specific expression of STEAP1, FXYD3, and FOLH1 (PSMA) and the NEPC-specific expression of NCAM1, SNAP25, and CEACAM5 were validated by immunoblot (Fig. 4A) and immunohistochemistry (IHC) (Fig. 4B) of prostate cancer cell lines and xenografts. Importantly, the expression patterns of these antigens in published human prostate cancer RNA-seq datasets mirrored the subtype-enriched expression observed in the cell-line panel (*SI Appendix, Fig. S3*). Flow cytometry confirmed the surface-protein expression of STEAP1 and FXYD3 on the LNCaP PrAd line, but not on the NCI-H660 NEPC line (Fig. 4C). Conversely, surface-protein expression of NCAM1 and CEACAM5 were found on NCI-H660, but not on LNCaP.

Validation of FXYD3 as a Tumor Antigen in PrAd. FXYD3 belongs to the FXYD family of regulators of Na⁺/K⁺ ATPases that contain a 35-amino acid signature sequence domain beginning with PFXYD (36). FXYD3 has previously been found to be overexpressed in a variety of cancers, including those of the breast, stomach, and pancreas (37–39). FXYD3 was strongly enriched in

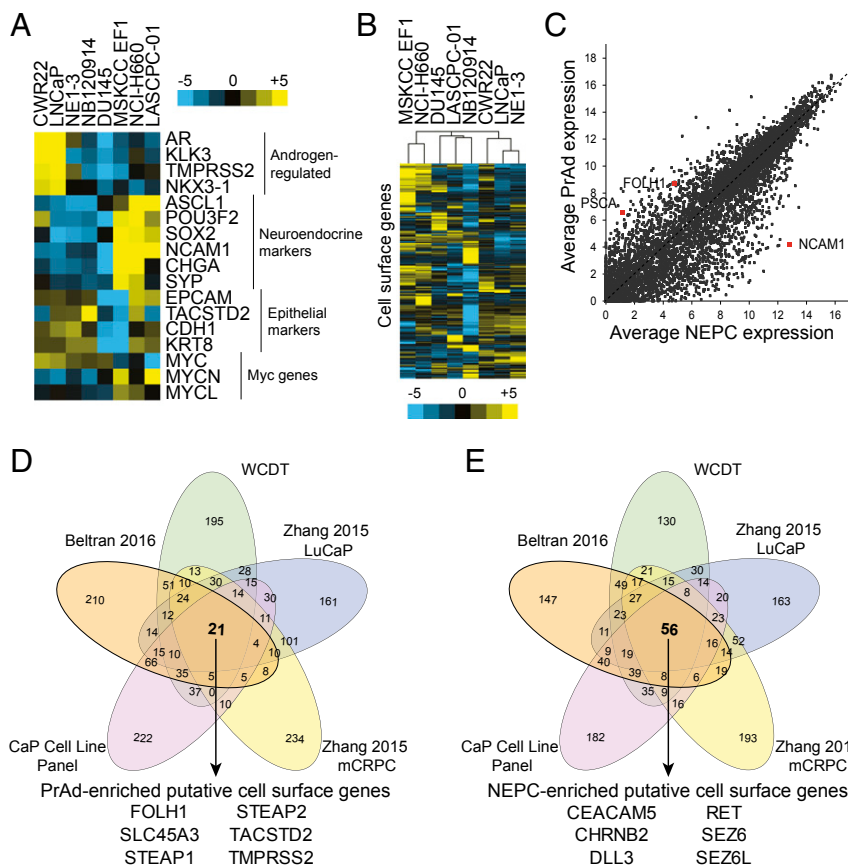


Fig. 2. Transcriptomic analysis identifies candidate PrAd- and NEPC-specific cell surface markers. (A) Heatmap of the gene expression of select androgen-regulated, neuroendocrine, and epithelial markers and Myc genes based on RNA-seq of a diverse panel of human prostate cancer cell lines. Color bar represents a log₂ scale. (B) Heatmap showing unsupervised hierarchical clustering of human prostate cancer cell lines based on the expression of cell-surface genes. (C) Plot of average expression of genes in NEPC vs. PrAd prostate cancer cell lines with select markers (NCAM1, FOLH1, and PSCA) highlighted. Gene expression is shown in log₂ scale. (D and E) Venn diagrams showing rank overlap of the top 500 differentially expressed cell-surface genes in PrAd relative to NEPC (D) and NEPC relative to PrAd (E) in each of five gene-expression datasets [prostate cancer (CaP) cell line panel, Beltran 2016, WCDT, Zhang 2015 LuCaP xenografts, and Zhang 2015 metastatic CRPC (mCRPC) samples]. Listed are the genes identified from rank overlap analysis that are enriched in all of the datasets evaluated.

the integrated transcriptomic and proteomic analysis in PrAd cell lines, but not as highly ranked by the transcriptome-based rank overlap analysis of the diverse prostate cancer datasets.

To evaluate FXYD3 expression in prostate cancer, we performed FXYD3 IHC on a tissue microarray of benign prostate samples as well as treatment-naïve primary Gleason grade 1–5 PrAd and metastatic PrAd. All 14 benign prostate tissues and 34 PrAd samples demonstrated FXYD3 expression (Fig. 5A), with the majority demonstrating moderate to strong staining specific to the normal and cancerous prostate epithelial cells (Fig. 5A and C). FXYD3 IHC was also performed on a series of small cell NEPC tissues archived at the University of California, Los Angeles (UCLA) (SI Appendix, Fig. S4). We found that in several samples with mixed PrAd and small-cell NEPC, FXYD3 appeared to be more highly expressed in the PrAd components of the tumors (Fig. 5B). Quantitation of the FXYD3 IHC scores in all evaluated samples showed that FXYD3 protein expression was reduced on average in small-cell NEPC relative to benign prostate and PrAd (Fig. 5C).

Evaluation of the NIH Genotype-Tissue Expression (GTEx) database showed that FXYD3 gene expression in human males is expressed in a variety of tissues including the skin, esophagus, stomach, small intestine, colon, bladder, and prostate (SI Appendix, Fig. S5A) (40). Congruent with the gene-expression data, IHC of a normal human tissue microarray demonstrated FXYD3 protein expression primarily in these organs (SI Appendix, Fig. S5B). The broad range of normal tissue expression would indicate that FXYD3 may not be suitable as a single target for highly potent cell-based immunotherapy due to the potential for on-target off-tumor toxicities. However, whether FXYD3 may be amenable to targeting by monoclonal antibodies or antibody drug conjugates (ADCs) is unknown, as dose-limiting off-tumor toxicity has not necessarily correlated with normal tissue expression (41).

Validation of CEACAM5 as a Target Antigen in NEPC. CEACAM5 was identified as a candidate NEPC target antigen by both transcriptomic analysis of diverse prostate cancer datasets (Fig. 2E) and by integrated transcriptomic and proteomic analysis of the prostate cancer cell lines (Fig. 3C). In support of these findings, coexpression analysis of the Beltran 2016 dataset identified that the gene expression of CEACAM5 is highly correlated with the neuroendocrine marker chromogranin A (SI Appendix, Fig. S3B) (14). A similar, strong correlation was also found between CEACAM5 and the proneural pioneer transcription factor and high-grade neuroendocrine carcinoma marker ASCL1 in a metastatic prostate cancer gene-expression dataset (SI Appendix, Fig. S3C) (42, 43). CEACAM5 (CEA or carcinoembryonic antigen) is a glycosphosphatidylinositol-anchored membrane protein and established tumor antigen whose expression has primarily been associated with adenocarcinomas of the colon, rectum, and pancreas. Despite case reports of detectable serum CEA in rare patients with advanced prostate cancer, a systematic study of CEACAM5 IHC in prostate tumors identified no expression in both primary and metastatic samples (44).

To verify protein expression of CEACAM5 in NEPC, we performed IHC on a prostate cancer tissue microarray of the LuCaP series of PDX models (45). While the 13 androgen-sensitive PrAd PDXs and 9 castration-resistant PrAd PDXs evaluated did not demonstrate CEACAM5 expression, all 4 NEPC PDXs exhibited moderate or strong CEACAM5 staining localized to the plasma membrane (Fig. 6A). We extended the IHC evaluation of CEACAM5 expression to a series of small-cell NEPC tissues archived at UCLA and a tissue microarray of benign prostate samples, as well as treatment-naïve primary Gleason grade 1–5 PrAd and metastatic PrAd. Eleven of 18 (61.1%) of the small-cell NEPC tissues stained for CEACAM5 in the plasma membrane (Fig. 6B and C and SI Appendix, Fig. S6). In contrast, all 14 benign prostate tissues and 34 PrAd samples encompassing primary and metastatic

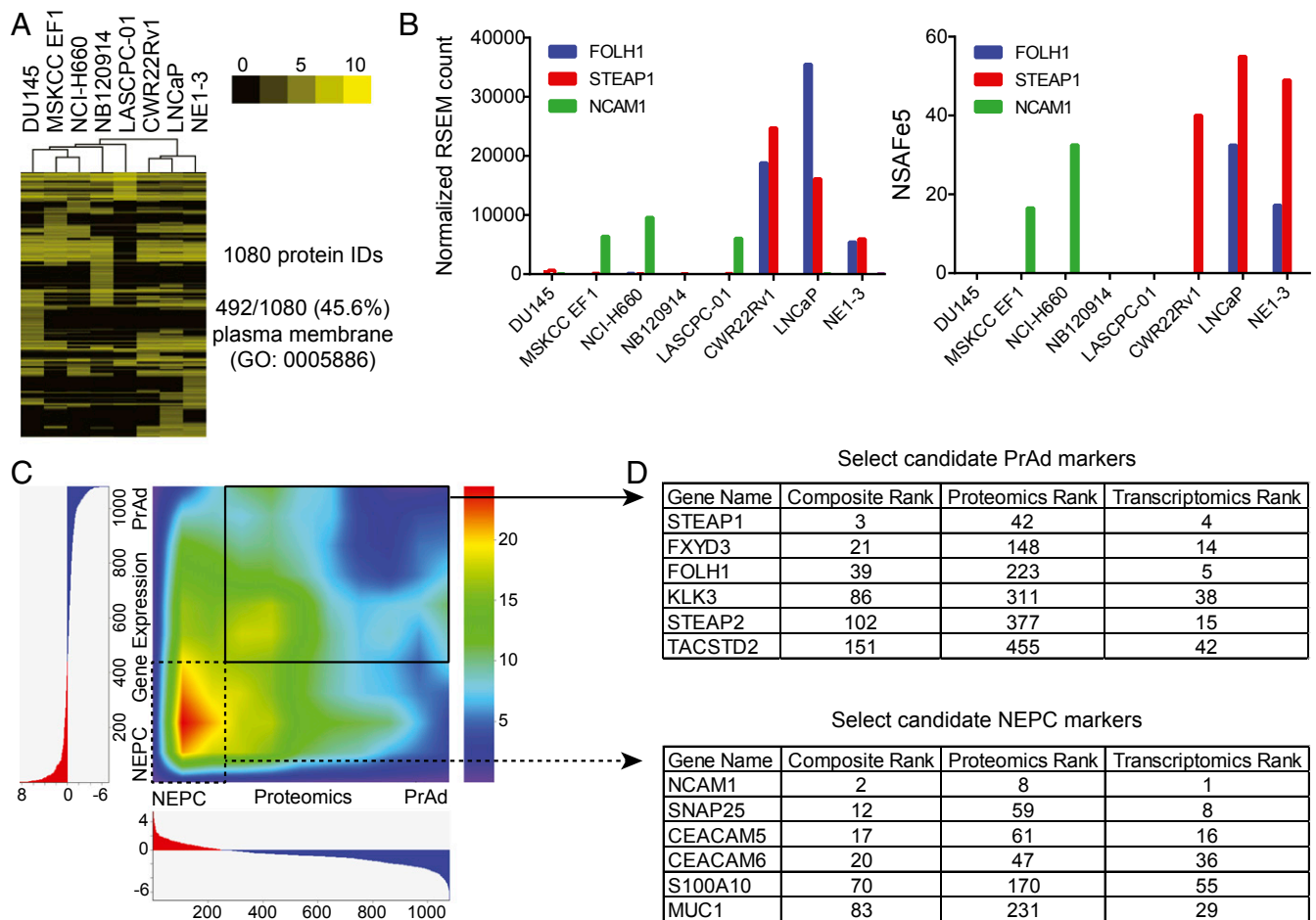


Fig. 3. Integration of cell-surface proteomics with transcriptomics nominates high-confidence PrAd and NEPC cell surface proteins. (A) Heatmap displaying unsupervised hierarchical clustering of prostate cancer cell lines based on the expression of cell-surface proteins identified from cell-surface proteomics. Depicted are normalized protein abundance values (NSAF₅). Color bar represents a log₂ scale. GO, Gene Ontology. (B) Comparison of the normalized RSEM gene expression counts and NSAF₅ values for the cell-surface markers FOLH1, STEAP1, and NCAM1 in each of the prostate cancer cell lines. (C) Rank–rank hypergeometric heatmap showing rank overlap of differentially expressed cell-surface proteins vs. cell-surface genes identified from cell-surface proteomics and RNA-seq gene-expression analysis of the prostate cancer cell line panel. (D) Select markers demonstrating concordantly enriched protein and gene expression in the PrAd or NEPC cell lines are shown with their associated composite, proteomics, and transcriptomics ranks.

tissues were devoid of CEACAM5 immunoreactivity (*SI Appendix, Fig. S7*). These IHC validation studies indicate that CEACAM5 expression appears to be prevalent in and specific to the NEPC subtype of prostate cancer.

Therapeutic Targeting of CEACAM5 in NEPC. CEACAM5 is an antigen that is the active focus of therapeutic development in colorectal cancer with ADCs and CAR T cells (46, 47). Given our findings, we sought to examine the potential for CEACAM5-targeted therapy in NEPC. We first explored safety implications by examining the systemic expression of CEACAM5 in normal human tissues at the mRNA and protein levels. Evaluation of the NIH GTEx database showed that CEACAM5 gene expression in men is limited to the colon, esophagus, and small intestine (*SI Appendix, Fig. S8A*) (40). A previous study of adoptive cell therapy with T cells engineered to express a high-affinity murine T cell receptor (TCR) targeting CEACAM5 in patients with metastatic colorectal cancer reported tumor regression, but also severe, transient colitis (48). However, data from a phase I trial of CEA-directed CAR T cell immunotherapy in CEA-positive metastatic colorectal cancers have indicated that CEA CAR T cell therapy may be well tolerated without evidence of colitis, even at high doses (47). In concordance with gene-expression data from the GTEx database, immunoblot

analysis of a range of human tissue lysates from vital organs revealed absence of CEACAM5 protein expression in the brain, heart, kidney, liver, and lung (Fig. 4A). In addition, IHC of a normal human tissue microarray demonstrated CEACAM5 expression limited to the luminal lining of the colon and rectum in men (*SI Appendix, Fig. S8B*).

Given the relatively restricted systemic expression of CEACAM5 and the highly aggressive clinical nature of NEPC, we chose to engineer CARs targeting CEACAM5 to leverage both antigen specificity and cytotoxic potency of this technology. We generated two lentiviral CEACAM5 CAR constructs encoding a single chain variable fragment (scFv) derived from labetuzumab (49), hinge/spacer, CD28 transmembrane domain, CD28 costimulatory domain, and CD3ζ activation domain (Fig. 7A). The CEACAM5 CARs differed based on the presence of either a short spacer (IgG4 hinge) or long spacer (IgG4 hinge and CH2+CH3 spacer). We transduced T cells expanded from human peripheral blood mononuclear cells (PBMCs) with the CAR constructs and performed coculture assays with the target NEPC cell lines MSKCC EF1 (CEACAM5-negative; Fig. 4A and B), MSKCC EF1-CEACAM5 (engineered to express CEACAM5), and NCI-H660 (CEACAM5-positive; Fig. 4) at a fixed effector-to-target ratio of 1:1. Analysis of the supernatant at 12 and 24 h by IFN-γ ELISA revealed enhanced antigen-specific IFN-γ release associated with

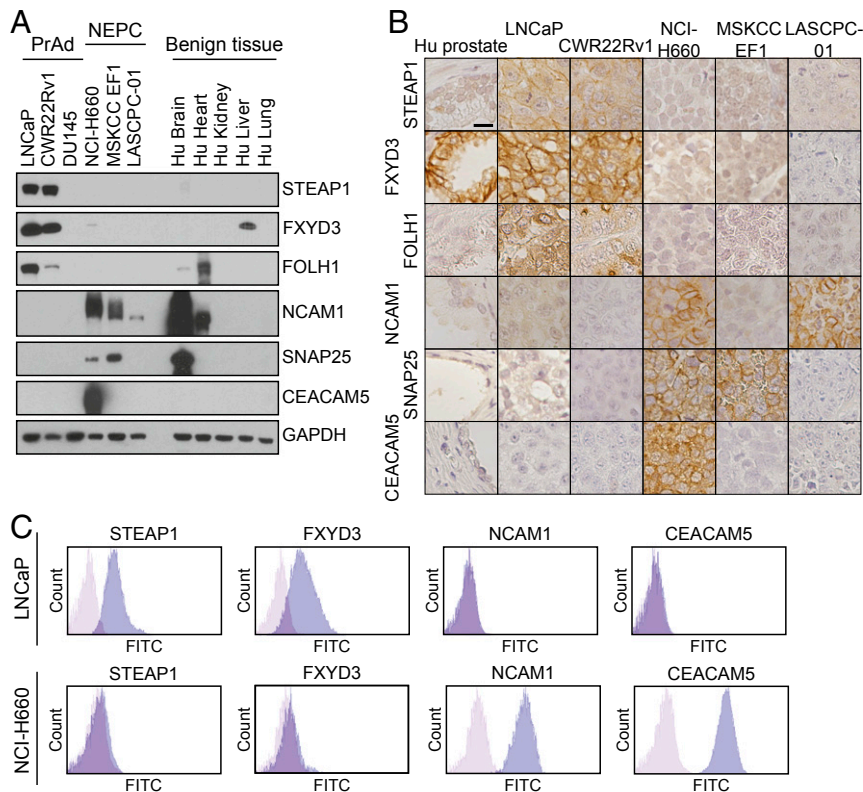


Fig. 4. Validation of candidate prostate cancer subtype-specific cell-surface antigens. (A) Immunoblot analysis of select PrAd (LNCaP, CWR22Rv1, and DU145) and NEPC (NCI-H660, MSKCC EF1, and LASCPC-01) cell lines as well as benign human tissues (brain, heart, kidney, liver, and lung) with antibodies against STEAP1, FXYD3, FOLH1, NCAM1, SNAP25, CEACAM5, and GAPDH as a loading control. (B) Human prostate tissue (Hu prostate) or prostate cancer cell line (LNCaP, CWR22Rv1, NCI-H660, MSKCC EF1, and LASCPC-01) xenograft sections after immunohistochemical staining with antibodies for the candidate antigens from A. (Scale bar, 25 μ m.) (C) Flow cytometry histogram plots of the PrAd cell line LNCaP and the NEPC cell line NCI-H660 stained with antibodies against STEAP1, FXYD3, NCAM1, and CEACAM5.

the long spacer CEACAM5 CAR (Fig. 7B). As the A3B3 domain of CEACAM5 recognized by the scFv is proximal to the membrane, a longer spacer may be necessary for optimal binding and T cell activation (49, 50).

To quantify cytotoxicity, we performed coculture assays in an Incucyte ZOOM (51), a live-cell imaging and analysis system allowing for direct enumeration of effector and target cells based on bright-field and fluorescence imaging. Varying effector-to-target ratios of T cells transduced with the long spacer CEACAM5 CAR and either MSKCC EF1 (CEACAM5-negative) or NCI-H660 (CEACAM5-positive) target NEPC cell lines engineered to express green fluorescent protein (GFP) were cocultured. Target cell counts were calculated and plotted to show relative target cell viability over time in coculture with effector cells. Coculture of long spacer CEACAM5 CAR-transduced T cells with NCI-H660 led to >80–90% cell kill by 48 h at effector-to-target ratios of 1:1 and 2:1 (Fig. 7C). In contrast, coculture with the MSKCC EF1 caused a minor reduction in target cell viability by 48 h, which may be related to low levels of CEACAM5 expression in the MSKCC EF1 NEPC cell line. Similar coculture studies were also performed with the PrAd cell line DU145 (CEACAM5-negative) and DU145-CEACAM5 (engineered to express CEACAM5). Long spacer CEACAM5 CAR-transduced T cells had negligible effects on the DU145 cells but induced significant T cell activation and target cell death when cocultured with DU145-CEACAM5 cells (*SI Appendix, Fig. S9 A and B*). These findings provide preliminary support for CEACAM5 as a promising target antigen for further therapeutic development in NEPC.

Discussion

Therapeutic development for advanced prostate cancer has increased significantly over the last decade. Both antibody- and cell-based immune treatment strategies are now poised to advance to the clinic, as monoclonal antibodies, ADCs, and CAR T cells are under clinical investigation. Most of these prospective therapies are focused on PSMA and PSCA as target antigens in CRPC. However, the heterogeneity of CRPC and the potential for treatment-induced plasticity (6, 52, 53) indicate that agents targeting only PSMA and PSCA are unlikely to eradicate the disease. An additional complication is the paucity of cancer-specific antigens that are not expressed in normal tissues (54). Sequential or combinatorial treatment strategies targeting distinct antigens while optimizing safety at various stages of disease progression will likely be necessary (55). To this end, we have characterized the surfaceome of advanced prostate cancer and generated a collection of putative target antigens using a discovery pipeline based on mRNA and cell-surface protein expression data. These studies are relevant and timely with the intent of expanding the development of targeted biologic therapies for advanced prostate cancer.

We have identified significant biological differences between the PrAd and NEPC subsets based on cell-surface protein profiling. Our data indicate that PrAd and NEPC express distinct cell-surface markers that mirror their respective glandular epithelial and neuroendocrine cancer differentiation states. Global cell-surface gene-expression analysis of these subsets across multiple published prostate cancer datasets clearly indicate that the surface phenotype of NEPC is more conserved than that of PrAd. This finding is consistent with the observed heterogeneity of PrAd that demonstrates a broad spectrum of histologic

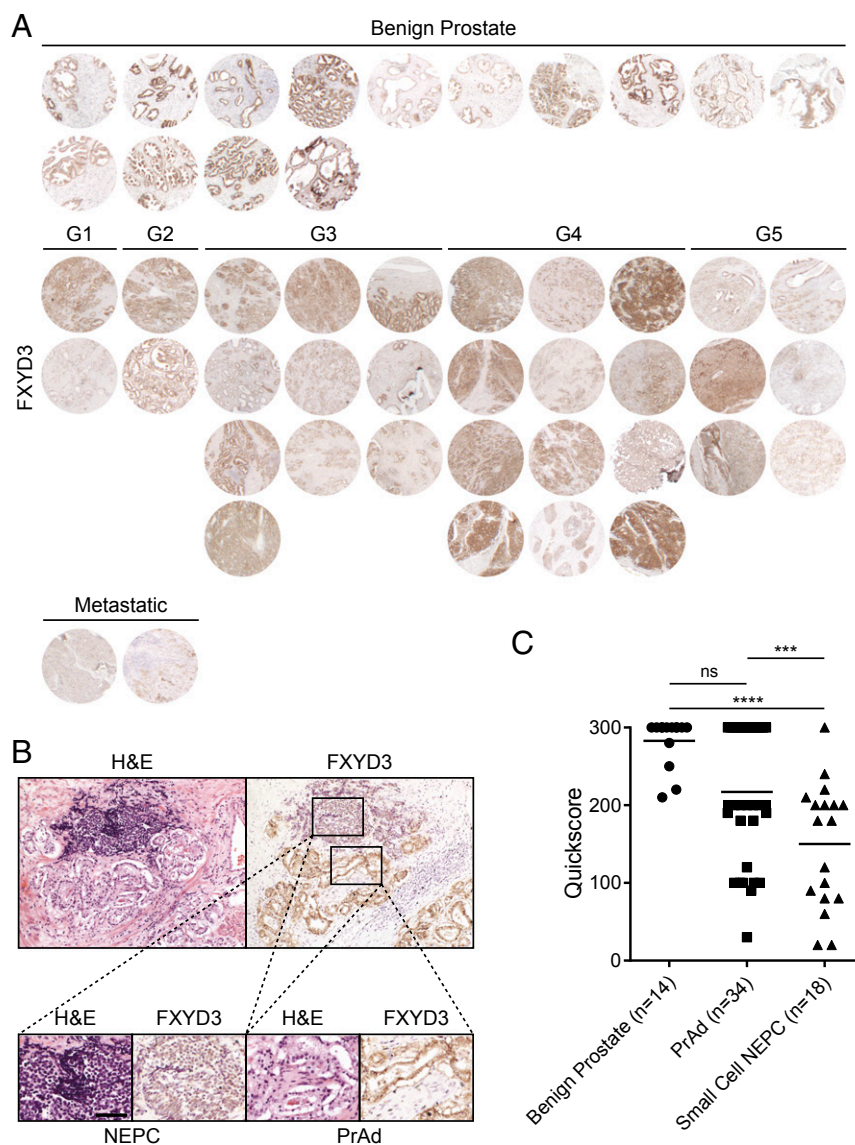


Fig. 5. FXYD3 is a cell-surface antigen whose expression is enriched in benign prostate epithelial cells and PrAd. (A) FXYD3 immunohistochemical stains of benign prostate tissues ($n = 14$), primary Gleason grade 1–5 PrAd tissues ($n = 32$), and metastatic PrAd samples ($n = 2$). (B) H&E and FXYD3 immunohistochemical stains of a section of mixed PrAd and NEPC. (Scale bar, 200 μm .) (C) Quantitation of FXYD3 IHC in benign prostate tissues ($n = 14$), PrAd ($n = 34$), and small-cell NEPC samples ($n = 18$) by Quickscore (intensity \times percentage of positive cells; maximum score is 300). ns, nonsignificance. $**P < 0.01$; $****P < 0.0001$ (by one-way ANOVA statistical analysis).

features, molecular subtypes, and clinical behaviors. On the other hand, the cell-surface profile of NEPC appears relatively homogeneous, suggesting that transdifferentiation to NEPC may represent a phenotypically constraining evolutionary path.

To nominate specific target antigens in prostate cancer as potential immunotherapeutic targets for further validation, cell-surface gene-expression and proteomics data were integrated from a diverse panel of prostate cancer cell lines. However, a pitfall of this approach is that mRNA abundance does not necessarily correlate with protein abundance (56), likely due to posttranscriptional and post-translational modifications affecting stability. In the future, technological improvements in ultrasensitive quantitative mass spectrometry in proteomics may obviate the need to consider mRNA data and enable global surfaceome analysis for target antigen discovery directly from biopsy specimens. Another limitation in the validation and therapeutic translation of candidate target antigens is the availability of specific immunoaffinity reagents against extracellular protein domains. Large-scale efforts to characterize the expression

of all human proteins in both normal and cancerous cells and tissues have been fraught with issues of data reliability due to inconsistent antibody performance (57). However, advances in recombinant antibody production including the use of highly diverse phage display and antibody library technologies should help overcome this bottleneck (58, 59).

We have specifically demonstrated that FXYD3 and CEACAM5 are plasma membrane-bound antigens expressed preferentially in PrAd and NEPC, respectively, based on multilevel validation studies on prostate cancer cell lines and tissues. We evaluated the normal tissue expression of these antigens as an additional filter to determine the potential for off-tumor, on-target toxicities of antibodies or cell-based immunotherapies. Due to the clinical need for novel therapies for aggressive NEPC, combined with our characterization of CEACAM5 expression in NEPC (including small-cell prostate cancer) and normal tissues, we have engineered CEACAM5 CAR constructs and demonstrated their potent antigen-specific NEPC cytotoxicity. CEACAM5 is

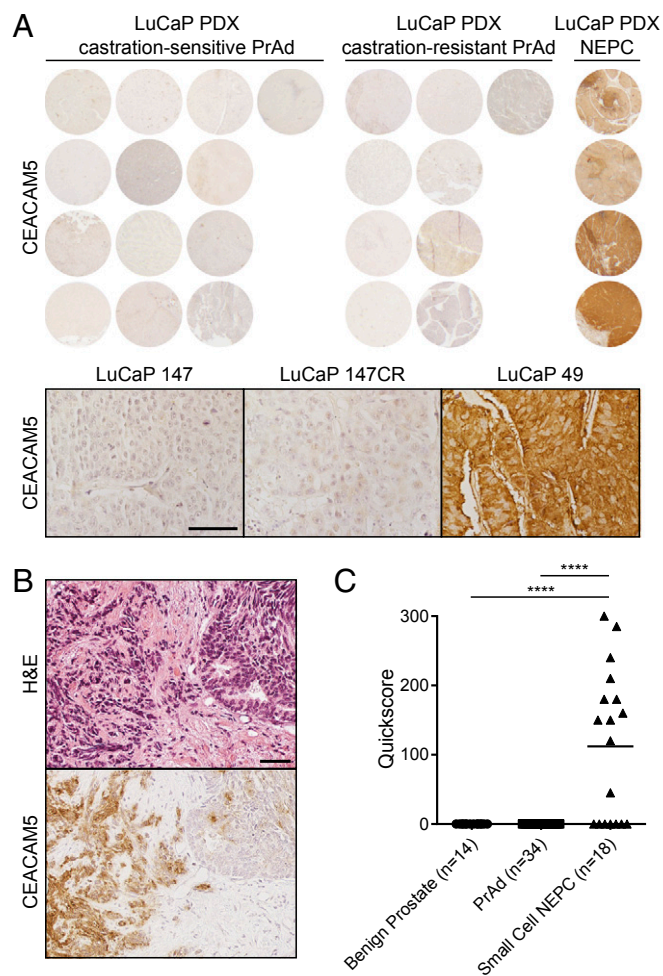


Fig. 6. CEACAM5 is a prostate cancer cell-surface antigen specific to the NEPC subtype. (A) CEACAM5 IHC of a LuCaP PDX tissue microarray with androgen-sensitive PrAd samples ($n = 13$), castration-resistant PrAd samples ($n = 9$), and NEPC samples ($n = 4$). CEACAM5 immunohistochemical stains of representative androgen-sensitive PrAd (LuCaP 147), castration-resistant PrAd (LuCaP 147CR), and NEPC (LuCaP 49) sections. (Scale bar, 100 μm .) (B) H&E and CEACAM5 immunohistochemical stains of a small cell NEPC sample archived at UCLA demonstrating adjoining regions of small-cell NEPC (left) and PrAd (right). (Scale bar, 100 μm .) (C) Quantitation of CEACAM5 IHC in benign prostate tissues ($n = 14$), PrAd ($n = 34$), and small-cell NEPC samples ($n = 18$) by Quickscore (intensity \times percentage of positive cells; maximum score is 300). **** $P < 0.0001$ (by one-way ANOVA statistical analysis).

an attractive therapeutic target in several solid tumors, but the translation of CEACAM5-targeted therapies is overwhelmingly focused on advanced colorectal cancer. A number of immune-based strategies have shown preclinical efficacy and are under clinical investigation, including antibody–drug conjugates (46, 60), a CEACAM5 and CD3 bispecific antibody (61), adoptive TCR transfer (48), and CAR T immunotherapy (47).

Our preliminary results indicate that CEACAM5-directed CAR T immunotherapy warrants further investigation as a treatment strategy for NEPC. Future studies will need to assess the antitumor efficacy and potential for toxicity in the gastrointestinal tract (48) in relevant, immune-competent model systems. Additionally, strategies to enhance the specificity and alleviate potential off-tumor toxicity of CEACAM5 CARs in NEPC should also be explored. One such approach is to use dual-gate CARs (62), in which two CARs, one targeting CEACAM5 and the other a second tumor antigen with nonoverlapping expression with CEACAM5 in normal tissues, are coexpressed in T cells

such that each individual CAR is insufficient to induce a T cell response, but when both CARs are engaged, they synergize to promote T cell activation. Lastly, CARs targeting PSCA or PSMA and CEACAM5 either together or as a single bispecific construct (63) should be evaluated for safety and efficacy as a strategy to address the heterogeneity of advanced CRPC.

Methods

Detailed descriptions of cell lines, mouse xenograft studies, prostate cancer tissue microarrays and sections, antibodies, IHC, flow cytometry, and lentiviral vectors are found in *SI Appendix, SI Methods*. Viable human cells and tissues were provided in a deidentified manner and were therefore exempt from Institutional Review Board approval. All animal studies were performed according to protocols approved by the Animal Research Committee at University of California, Los Angeles.

Bioinformatic Derivation of Genes Encoding the Cell Surfaceome. Genes encoding cell-surface proteins were assembled based on Gene Ontology annotations (22) (Membrane, Plasma Membrane, Integral Components of the Membrane, and Integral Components of the Plasma Membrane), putative transmembrane proteins based on analysis of the UniProt proteome of *Homo sapiens* using TMHMM (Version 2.0) (23), and predictions of GPI-anchored proteins from PredGPI (64).

RNA-Seq. RNA was isolated from human prostate cancer cell lines by using an miRNeasy Mini Kit (Qiagen). Libraries for RNA-seq were prepared by using a TruSeq RNA Library Prep Kit (Version 2; Illumina). Sequencing was performed on an Illumina HiSeq 3000 with 2×150 -bp reads. Demultiplexing of reads was performed by using CASAVA software (Version 1.8.2; Illumina). The Toil RNA-Seq Pipeline developed by the Computational Genomics Laboratory at the Genomics Institute of the University of California, Santa Cruz, was run locally to obtain gene- and transcript-level RSEM quantification of expression (65).

Transcriptome Analysis. FASTQ files from the Beltran 2016 RNA-Seq dataset were downloaded from dbGaP (study accession no. phs000909.v1.p1) and analyzed with the Toil RNA-Seq Pipeline. The TCGA and NIH GTEx Toil RNAseq Recompute datasets were downloaded from the University of California, Santa Cruz, Xena Public Data Hub (65). In each prostate cancer gene expression dataset analyzed, differentially expressed cell-surface genes between NEPC and PrAd samples [false discovery rate (FDR) < 0.05] were ranked based on the magnitude of fold change. RRHO analysis was performed in pairwise comparisons of gene-expression datasets as described (25). For PANTHER analysis, cell-surface genes enriched more than eightfold in either NEPC or PrAd samples in the Beltran 2016 dataset were submitted for overrepresentation testing as described (27). Rank overlap analysis was performed by taking the 500 most differentially enriched cell-surface genes in NEPC and PrAd samples from each dataset (FDR < 0.05) and identifying genes similarly enriched across all datasets.

Proteomic Analysis. A total of 4×10^7 cells from each cell line were subjected to cell-surface biotinylation and quenching per the Pierce Cell Surface Protein Isolation Kit (Thermo Fisher Scientific). Cells were lysed in urea lysis buffer (8 M urea, 2% SDS, and 100 mM Tris, pH 8) and DNA digested with 250 U of Benzonase endonuclease (Sigma). Biotin-labeled proteins were affinity-purified on streptavidin agarose beads (Thermo Fisher Scientific), sequentially treated with 5 mM Tris(2-carboxyethyl) phosphine and 10 mM iodoacetamide, and digested on-bead with Lys-C and trypsin proteases as described (66). Peptides were fractionated by multidimensional chromatography followed by tandem mass spectrometric analysis on a LTQ-Orbitrap mass spectrometer (Thermo Fisher Scientific). RAW-Xtract (Version 1.8) was used to extract peak list information from Xcalibur-generated RAW files. Database searching of the MS/MS spectra was performed by using the ProLuCID algorithm (Version 1.0). Other database search parameters included (i) precursor ion mass tolerance of ± 20 ppm; (ii) fragment ion mass tolerance of ± 400 ppm; (iii) only peptides with fully tryptic ends were considered candidate peptides in the search with no consideration for missed cleavages; and (iv) static modification of +57.02156 on cysteine residues. Peptide identifications were organized and filtered by using the DTASelect algorithm, which uses a linear discriminant analysis to identify peptide-scoring thresholds that yield a peptide-level FDR of $< 5\%$ as estimated by using a decoy database approach. Proteins were considered present in the analysis if they were identified by two or more peptides using the 5% peptide-level FDR.

5. Kleb B, et al. (2016) Differentially methylated genes and androgen receptor re-expression in small cell prostate carcinomas. *Epigenetics* 11:184–193.
6. Ku SY, et al. (2017) Rb1 and Trp53 cooperate to suppress prostate cancer lineage plasticity, metastasis, and antiandrogen resistance. *Science* 355:78–83.
7. Beltran H, et al. (2011) Molecular characterization of neuroendocrine prostate cancer and identification of new drug targets. *Cancer Discov* 1:487–495.
8. Lee JK, et al. (2016) N-Myc drives neuroendocrine prostate cancer initiated from human prostate epithelial cells. *Cancer Cell* 29:536–547.
9. Dardenne E, et al. (2016) N-Myc induces an EZH2-mediated transcriptional program driving neuroendocrine prostate cancer. *Cancer Cell* 30:563–577.
10. Komura K, et al. (2018) Current treatment strategies for advanced prostate cancer. *Int J Urol* 25:220–231.
11. Afshar-Oromieh A, et al. (2014) Comparison of PET imaging with a (68)Ga-labelled PSMA ligand and (18)F-choline-based PET/CT for the diagnosis of recurrent prostate cancer. *Eur J Nucl Med Mol Imaging* 41:11–20.
12. Chakraborty PS, et al. (2015) Metastatic poorly differentiated prostatic carcinoma with neuroendocrine differentiation: Negative on 68Ga-PSMA PET/CT. *Clin Nucl Med* 40:e163–e166.
13. Tosoian JJ, et al. (2017) Correlation of PSMA-targeted ¹⁸F-DCFPyL PET/CT findings with immunohistochemical and genomic data in a patient with metastatic neuroendocrine prostate cancer. *Clin Genitourin Cancer* 15:e65–e68.
14. Beltran H, et al. (2016) Divergent clonal evolution of castration-resistant neuroendocrine prostate cancer. *Nat Med* 22:298–305.
15. DeVeale B, et al. (2014) Surfaceome profiling reveals regulators of neural stem cell function. *Stem Cells* 32:258–268.
16. Hofmann A, et al. (2010) Proteomic cell surface phenotyping of differentiating acute myeloid leukemia cells. *Blood* 116:e26–e34.
17. Maloney DG, et al. (1997) IDEC-C2B8 (rituximab) anti-CD20 monoclonal antibody therapy in patients with relapsed low-grade non-Hodgkin's lymphoma. *Blood* 90:2188–2195.
18. Kalos M, et al. (2011) T cells with chimeric antigen receptors have potent antitumor effects and can establish memory in patients with advanced leukemia. *Sci Transl Med* 3:95ra73.
19. Brentjens RJ, et al. (2013) CD19-targeted T cells rapidly induce molecular remissions in adults with chemotherapy-refractory acute lymphoblastic leukemia. *Sci Transl Med* 5:177ra38.
20. Sadelain M, Brentjens R, Rivière I (2013) The basic principles of chimeric antigen receptor design. *Cancer Discov* 3:388–398.
21. da Cunha JP, et al. (2009) Bioinformatics construction of the human cell surfaceome. *Proc Natl Acad Sci USA* 106:16752–16757.
22. Ashburner M, et al.; The Gene Ontology Consortium (2000) Gene ontology: Tool for the unification of biology. *Nat Genet* 25:25–29.
23. Sonnhammer EL, von Heijne G, Krogh A (1998) A hidden Markov model for predicting transmembrane helices in protein sequences. *Proc Int Conf Intell Syst Mol Biol* 6:175–182.
24. Zhang X, et al. (2015) SRRM4 expression and the loss of REST activity may promote the emergence of the neuroendocrine phenotype in castration-resistant prostate cancer. *Clin Cancer Res* 21:4698–4708.
25. Plaisier SB, Taschereau R, Wong JA, Graeber TG (2010) Rank-rank hypergeometric overlap: Identification of statistically significant overlap between gene-expression signatures. *Nucleic Acids Res* 38:e169.
26. Aggarwal R, et al. (2016) Targeting adaptive pathways in metastatic treatment-resistant prostate cancer: Update on the Stand Up 2 Cancer/Prostate Cancer Foundation-supported West Coast Prostate Cancer Dream Team. *Eur Urol Focus* 2:469–471.
27. Mi H, Muruganujan A, Casagrande JT, Thomas PD (2013) Large-scale gene function analysis with the PANTHER classification system. *Nat Protoc* 8:1551–1566.
28. Hong S-K, Kim J-H, Lin M-F, Park J-I (2011) The Raf/MEK/extracellular signal-regulated kinase 1/2 pathway can mediate growth inhibitory and differentiation signaling via androgen receptor downregulation in prostate cancer cells. *Exp Cell Res* 317:2671–2682.
29. Gao D, et al. (2014) Organoid cultures derived from patients with advanced prostate cancer. *Cell* 159:176–187.
30. Santoro M, et al. (1990) The ret proto-oncogene is consistently expressed in human pheochromocytomas and thyroid medullary carcinomas. *Oncogene* 5:1595–1598.
31. Saunders LR, et al. (2015) A DLL3-targeted antibody-drug conjugate eradicates high-grade pulmonary neuroendocrine tumor-initiating cells in vivo. *Sci Transl Med* 7:302ra136.
32. Waldmann J, et al. (2010) Microarray analysis reveals differential expression of benign and malignant pheochromocytoma. *Endocr Relat Cancer* 17:743–756.
33. Marguerat S, et al. (2012) Quantitative analysis of fission yeast transcriptomes and proteomes in proliferating and quiescent cells. *Cell* 151:671–683.
34. Elia G (2008) Biotinylation reagents for the study of cell surface proteins. *Proteomics* 8:4012–4024.
35. Nunomura K, et al. (2005) Cell surface labeling and mass spectrometry reveal diversity of cell surface markers and signaling molecules expressed in undifferentiated mouse embryonic stem cells. *Mol Cell Proteomics* 4:1968–1976.
36. Crambert G, Geering K (2003) FXYD proteins: New tissue-specific regulators of the ubiquitous Na,K-ATPase. *Sci STKE* 2003:RE1.
37. Morrison BW, et al. (1995) Mat-8, a novel phospholemman-like protein expressed in human breast tumors, induces a chloride conductance in *Xenopus* oocytes. *J Biol Chem* 270:2176–2182.
38. Kaye H, et al. (2006) FXYD3 is overexpressed in pancreatic ductal adenocarcinoma and influences pancreatic cancer cell growth. *Int J Cancer* 118:43–54.
39. Zhu ZL, et al. (2010) Expression and significance of FXYD-3 protein in gastric adenocarcinoma. *Dis Markers* 28:63–69.
40. GTEx Consortium (2013) The genotype-tissue expression (GTEx) project. *Nat Genet* 45:580–585.
41. Hinrichs MJ, Dixit R (2015) Antibody drug conjugates: Nonclinical safety considerations. *AAPS J* 17:1055–1064.
42. Alttre-Tacha D, Tyrrell J, Li F (2017) mASH1 is highly specific for neuroendocrine carcinomas: An immunohistochemical evaluation on normal and various neoplastic tissues. *Arch Pathol Lab Med* 141:288–292.
43. Kumar A, et al. (2016) Substantial interindividual and limited intraindividual genomic diversity among tumors from men with metastatic prostate cancer. *Nat Med* 22:369–378.
44. Blumenthal RD, Leon E, Hansen HJ, Goldenberg DM (2007) Expression patterns of CEACAM5 and CEACAM6 in primary and metastatic cancers. *BMC Cancer* 7:2.
45. Nguyen HM, et al. (2017) LuCaP prostate cancer patient-derived xenografts reflect the molecular heterogeneity of advanced disease and serve as models for evaluating cancer therapeutics. *Prostate* 77:654–671.
46. Dotan E, et al. (2017) Phase I/II trial of labezumab govitecan (anti-CEACAM5/SN-38 antibody-drug conjugate) in patients with refractory or relapsing metastatic colorectal cancer. *J Clin Oncol* 35:3338–3346.
47. Zhang C, et al. (2017) Phase I escalating-dose trial of CAR-T therapy targeting CEA+ metastatic colorectal cancers. *Mol Ther* 25:1248–1258.
48. Parkhurst MR, et al. (2011) T cells targeting carcinoembryonic antigen can mediate regression of metastatic colorectal cancer but induce severe transient colitis. *Mol Ther* 19:620–626.
49. Stein R, Goldenberg DM (2004) A humanized monoclonal antibody to carcinoembryonic antigen, labezumab, inhibits tumor growth and sensitizes human medullary thyroid cancer xenografts to dacarbazine chemotherapy. *Mol Cancer Ther* 3:1559–1564.
50. Guest RD, et al. (2005) The role of extracellular spacer regions in the optimal design of chimeric immune receptors: Evaluation of four different scFvs and antigens. *J Immunother* 28:203–211.
51. Artymovitch K, Appledorn DM (2015) A multiplexed method for kinetic measurements of apoptosis and proliferation using live-content imaging. *Methods Mol Biol* 1219:35–42.
52. Mu P, et al. (2017) SOX2 promotes lineage plasticity and antiandrogen resistance in TP53- and RB1-deficient prostate cancer. *Science* 355:84–88.
53. Miao L, et al. (2017) Disrupting androgen receptor signaling induces snail-mediated epithelial-mesenchymal plasticity in prostate cancer. *Cancer Res* 77:3101–3112.
54. Priceman SJ, Forman SJ, Brown CE (2015) Smart CARs engineered for cancer immunotherapy. *Curr Opin Oncol* 27:466–474.
55. Sadelain M, Rivière I, Riddell S (2017) Therapeutic T cell engineering. *Nature* 545:423–431.
56. Kosti I, Jain N, Aran D, Butte AJ, Sirota M (2016) Cross-tissue analysis of gene and protein expression in normal and cancer tissues. *Sci Rep* 6:24799.
57. Berglund L, et al. (2008) A gene-centric Human Protein Atlas for expression profiles based on antibodies. *Mol Cell Proteomics* 7:2019–2027.
58. Li K, et al. (2015) A fully human scFv phage display library for rapid antibody fragment reformatting. *Protein Eng Des Sel* 28:307–316.
59. Frenzel A, Schirrmann T, Hust M (2016) Phage display-derived human antibodies in clinical development and therapy. *MAbs* 8:1177–1194.
60. Bouillon-Pichault M, et al. (2017) Translational model-based strategy to guide the choice of clinical doses for antibody-drug conjugates. *J Clin Pharmacol* 57:865–875.
61. Bacac M, et al. (2016) A novel carcinoembryonic antigen T-cell bispecific antibody (CEA TCB) for the treatment of solid tumors. *Clin Cancer Res* 22:3286–3297.
62. Kloss CC, Condomines M, Cartellieri M, Bachmann M, Sadelain M (2013) Combinatorial antigen recognition with balanced signaling promotes selective tumor eradication by engineered T cells. *Nat Biotechnol* 31:71–75.
63. Zah E, Lin MY, Silva-Benedict A, Jensen MC, Chen YY (2016) T cells expressing CD19/CD20 bispecific chimeric antigen receptors prevent antigen escape by malignant B cells. *Cancer Immunol Res* 4:498–508.
64. Pierleoni A, Martelli PL, Casadio R (2008) PredGPI: A GPI-anchor predictor. *BMC Bioinformatics* 9:392.
65. Vivian J, et al. (2017) Toil enables reproducible, open source, big biomedical data analyses. *Nat Biotechnol* 35:314–316.
66. Oberholzer M, et al. (2011) Independent analysis of the flagellum surface and matrix proteomes provides insight into flagellum signaling in mammalian-infectious *Trypanosoma brucei*. *Mol Cell Proteomics* 10:M111.010538.

Supplementary Information for

Systemic surfaceome profiling identifies target antigens for immune-based therapy in subtypes of advanced prostate cancer

John K. Lee, Nathanael J. Bangayan, Timothy Chai, Bryan A. Smith, Tiffany E. Pariva, Sangwon Yun, Ajay Vashisht, Qingfu Zhang, Jung Wook Park, Eva Corey, Jiaoti Huang, Thomas G. Graeber, James Wohlschlegel, Owen N. Witte

Owen N. Witte

Email: owenwitte@mednet.ucla.edu

This PDF file includes:

SI Methods
Figs. S1 to S9
References for SI reference citations

Other supplementary materials for this manuscript include the following:

Datasets S1 to S2

SI Methods

Cell Lines. LNCaP, CWR22Rv1, and DU145 (ATCC) were grown in RPMI with 10% FBS. NCI-H660 (ATCC) and LASCPC-01 (1) were grown in HITES media containing RPMI, 5% FBS, 10 nM hydrocortisone, 10 nM beta-estradiol (Sigma), insulin-transferrin-selenium, and Glutamax (Life Technologies). NE1.3 (gift from J. Huang) was grown in RPMI with 10% charcoal-stripped serum. NB120814 was established from an intraoperative biopsy of metastatic prostate cancer at UCLA and grown in RPMI with 10% FBS. MSKCC EF1 was derived from the organoid line MSKCC-CaP4 (2) (gift from Y. Chen) and was grown in RPMI with 10% FBS.

Mouse Xenograft Studies. NSG (NOD-SCID-IL2R γ -null) mice were obtained from the Jackson laboratory and housed at UCLA animal facilities in accordance with the regulations of the Division of Laboratory Animal Medicine. 10⁶ cells from each prostate cancer cell line or 1 mm³ minced prostate tumor chunks were suspended in 75 μ l of cold Matrigel (BD Biosciences) and implanted subcutaneously into NSG mice. Xenograft tumors were harvested and fixed in 10% buffered formalin for 16 h.

Prostate Cancer Tissue Microarrays and Sections. Tissue microarrays used were human prostate disease spectrum arrays (US Biomax PR8011b), multi-normal human tissues arrays (US Biomax MNO1021), and LuCaP PDX models arrays (Prostate Cancer Biorepository Network). UCLA IRB approval (17-000148) was obtained to requisition cases of small cell NEPC archived by the Department of Pathology and Laboratory Medicine at UCLA. Blocks were sectioned by the Translational Pathology Core Laboratory at UCLA and all tissue slides made available to the investigators were devoid of patient identifiers.

Antibodies. Antibodies used were: anti-CK8 (Covance MMS-162P), anti-SYP (Novocastra NCL-SYNAP-299), anti-p63 (Santa Cruz 4A4), anti-AR (Santa Cruz N-20), anti-CHGA (Dako M0869), anti-STEAP (Santa Cruz B-4), anti-FXYD3 (LifeSpan Biosciences 2F7), anti-PSM (Santa Cruz F-2), anti-NCAM (Cell Signaling 3576), anti-SNAP25 (BioLegend SMI 81), anti-CEA (Dako II-7; Cell Signaling 2383), and anti-GAPDH (GeneTex GT239).

Immunohistochemistry. Formalin-fixed and paraffin-embedded tissue sections were deparaffinized in xylene and rehydrated in 100%, 95%, and 75% ethanol then PBS. Antigen retrieval was performed in 40 mM citrate buffer (pH 6) using a pressure cooker heated to 95 °C for 30 min. Tissue sections were blocked in 2.5% normal horse serum blocking solution (Vector Labs) and incubated overnight in primary antibody in a humidified chamber. Slides were washed with PBS and 0.1% Tween-20 (PBS-T), blocked with 3% hydrogen peroxide for 10 min, and washed again with PBS-T. Slides were incubated with anti-mouse HRP or anti-rabbit HRP antibodies (Vector Labs) for 1 h and stains visualized using DAB peroxidase substrate (Dako). Sections were counterstained with hematoxylin.

Flow Cytometry. LNCaP was non-enzymatically dissociated with Versene EDTA solution (Thermo Fisher Scientific). NCI-H660 was collected from suspension culture and dissociated mechanically by pipetting. Cell lines were washed with PBS and incubated in flow cytometry staining buffer (PBS with 2% FBS and 0.09% sodium azide) with primary antibody or isotype control antibodies for 1 h. Cells were washed with PBS and incubated with mouse or rabbit IgG (H+L) fluorescein-conjugated secondary antibody (R&D Systems) for 1 h. Cells were washed with PBS, resuspended in flow cytometry staining buffer, and analyzed on a BD FACSCanto (BD Biosciences).

Lentiviral Vectors. The third-generation lentiviral vector FU-CGW, derived from FUGW, was used to label target cell lines with GFP for co-culture experiments. Human CEACAM5 cDNA was cloned into FU-CGW by NEBuilder HiFi DNA Assembly (New England Biolabs) to generate the lentiviral vector FU-CEACAM5-CGW to express CEACAM5 in select target cell lines. The short spacer and longer spacer CEACAM5 CAR constructs were generated by NEBuilder HiFi DNA Assembly of custom gBlocks gene fragments (Integrated DNA Technologies) and cloned into FU-W. Lentiviruses were produced and titered as previously described (3).

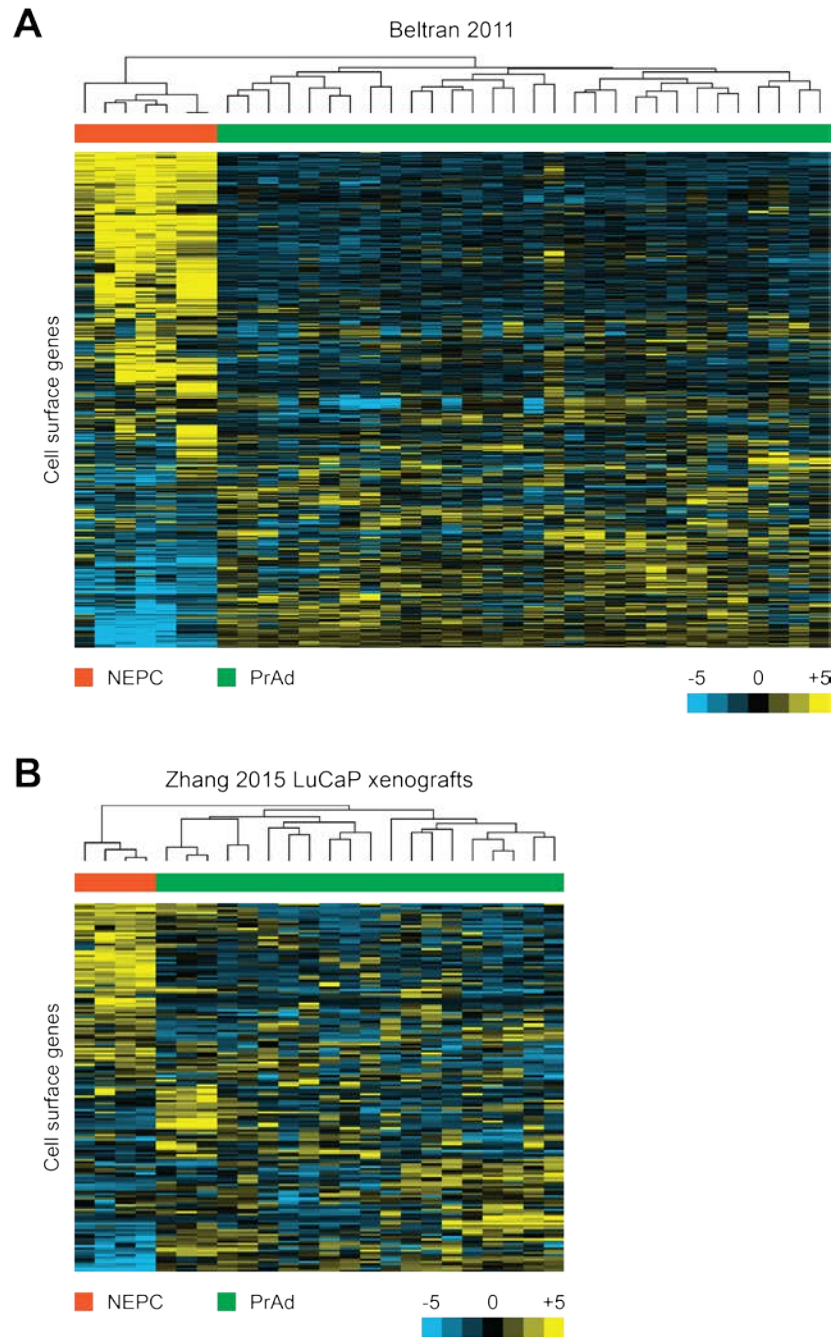


Fig. S1. Cell surface gene expression differentiates NEPC from PrAd. (A-B) Heatmaps demonstrating unsupervised hierarchical clustering of prostate cancer samples from the (A) Beltran 2011 RNA-seq dataset and (B) Zhang 2015 gene expression microarray dataset based on the expression of cell surface genes. Color bar represents a \log_2 scale. NEPC samples are labelled in orange and PrAd samples in green.

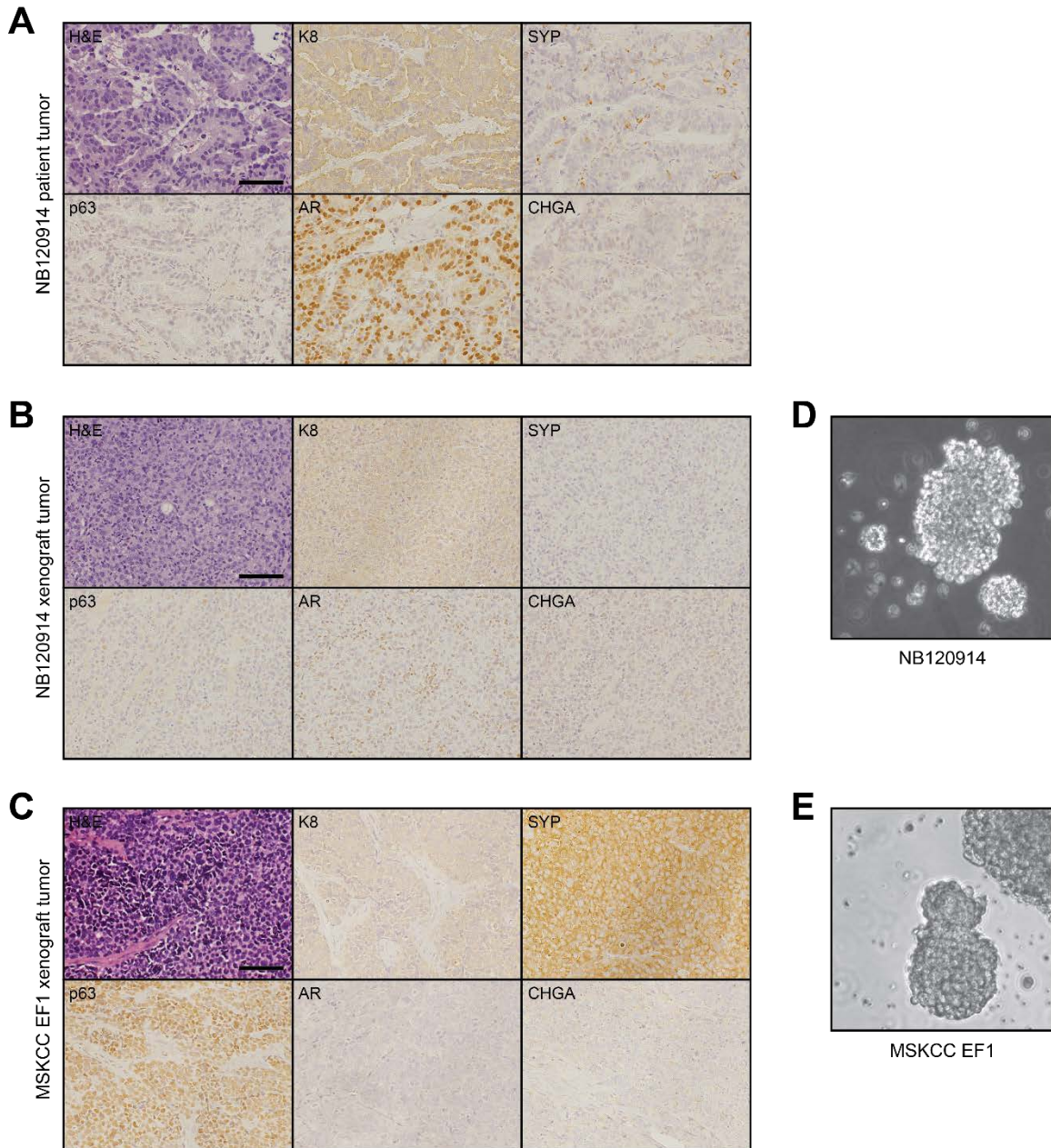


Fig. S2. Characterization of newly developed and adapted human prostate cancer cell lines. (A-C) H&E and K8, SYP, p63, AR, and CHGA immunohistochemical stains of the (A) NB120914 patient tumor, (B) NB120914 patient-derived xenograft tumor, and (C) MSKCC EF1 xenograft tumor. Scale bar represents 100 μ m. (D-E) Photomicrographs of the (D) NB120914 and (E) MSKCC EF1 cell lines in suspension culture growing in cell clusters.

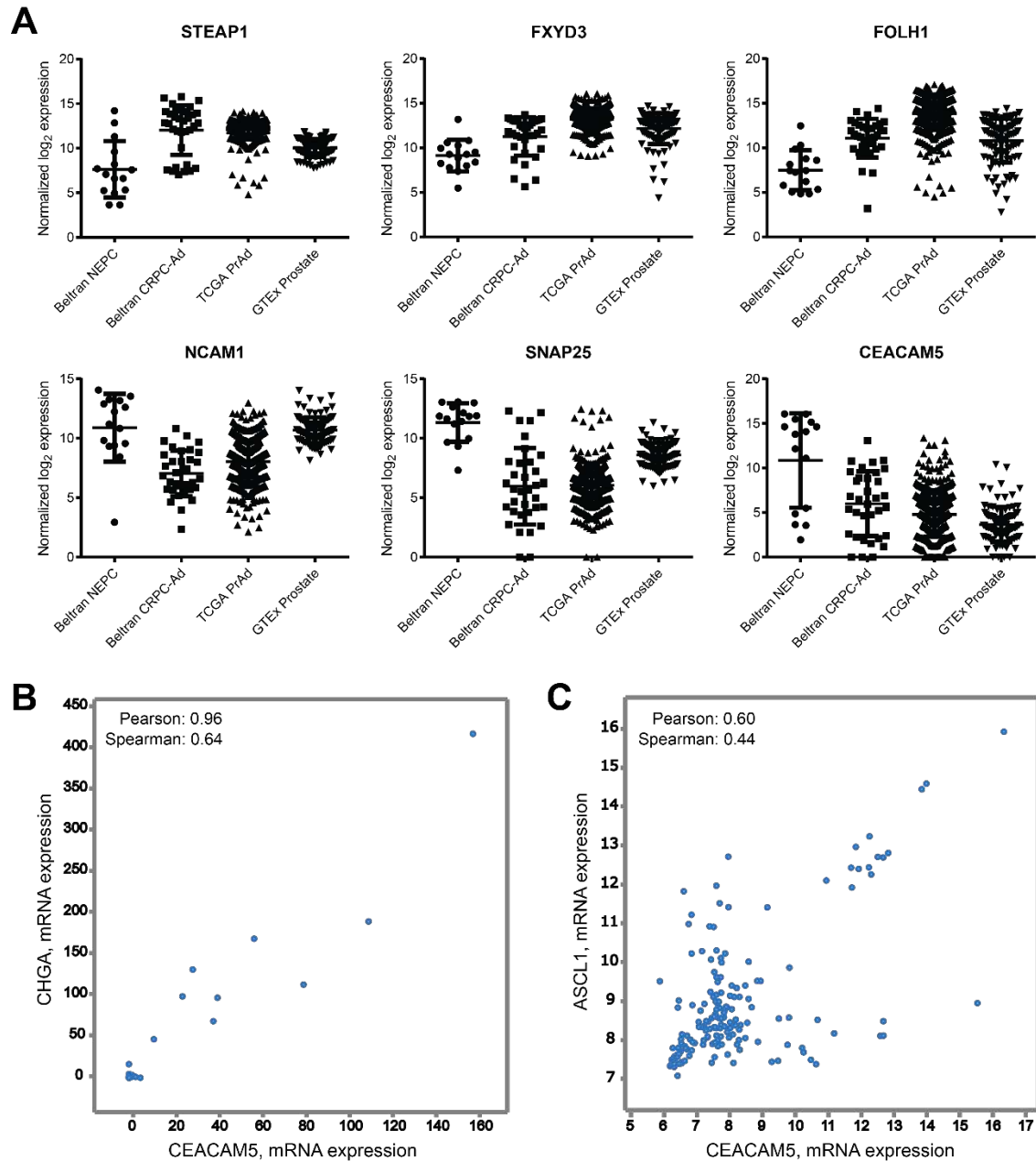


Fig. S3. Expression of candidate PrAd and NEPC cell surface antigens in prostate cancer and benign prostate gene expression datasets. (A) Vertical scatter plots of STEAP1, FXYD3, FOLH1, NCAM1, SNAP25, and CEACAM5 gene expression in NEPC and CRPC-Ad samples from Beltran 2016, primary prostate cancers from TCGA PrAd, and benign prostate tissues from the NIH GTEx dataset. Mean and standard deviation bars are also shown. (B-C) mRNA co-expression analysis from cBioPortal for Cancer Genomics showing correlation between (B) CEACAM5 and CHGA expression in the Trento/Cornell/Broad 2016 NEPC dataset and (C) CEACAM5 and ASCL1 in the Fred Hutchinson CRC, Nat. Med. 2016, dataset. Pearson and Spearman correlation coefficients are shown.

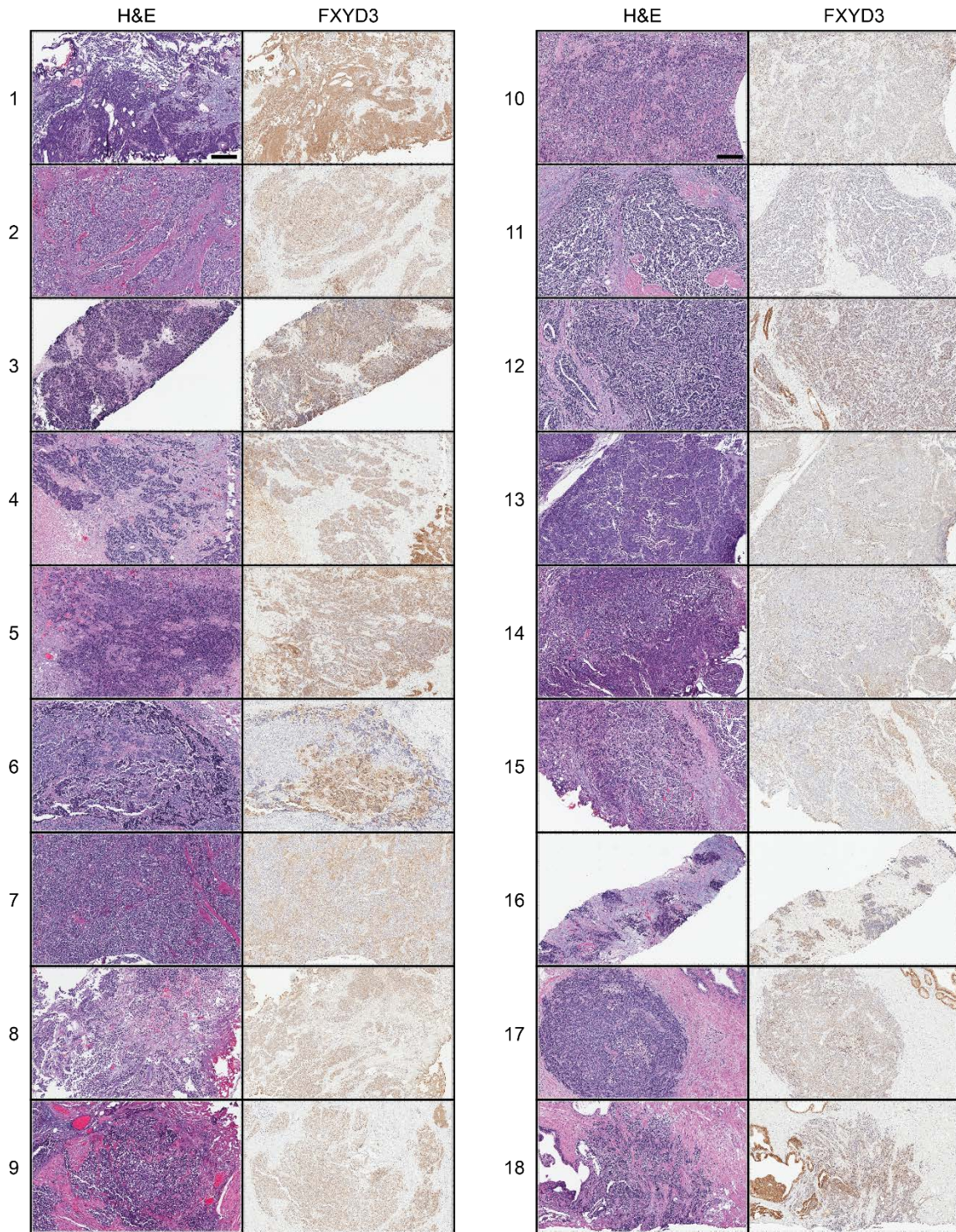


Fig. S4. Evaluation of FXYD3 expression in a series of small cell NEPC cases. H&E and FXYD3 immunohistochemical stains of 18 independent small cell NEPC samples archived at UCLA. Scale bar represents 200 μ m.

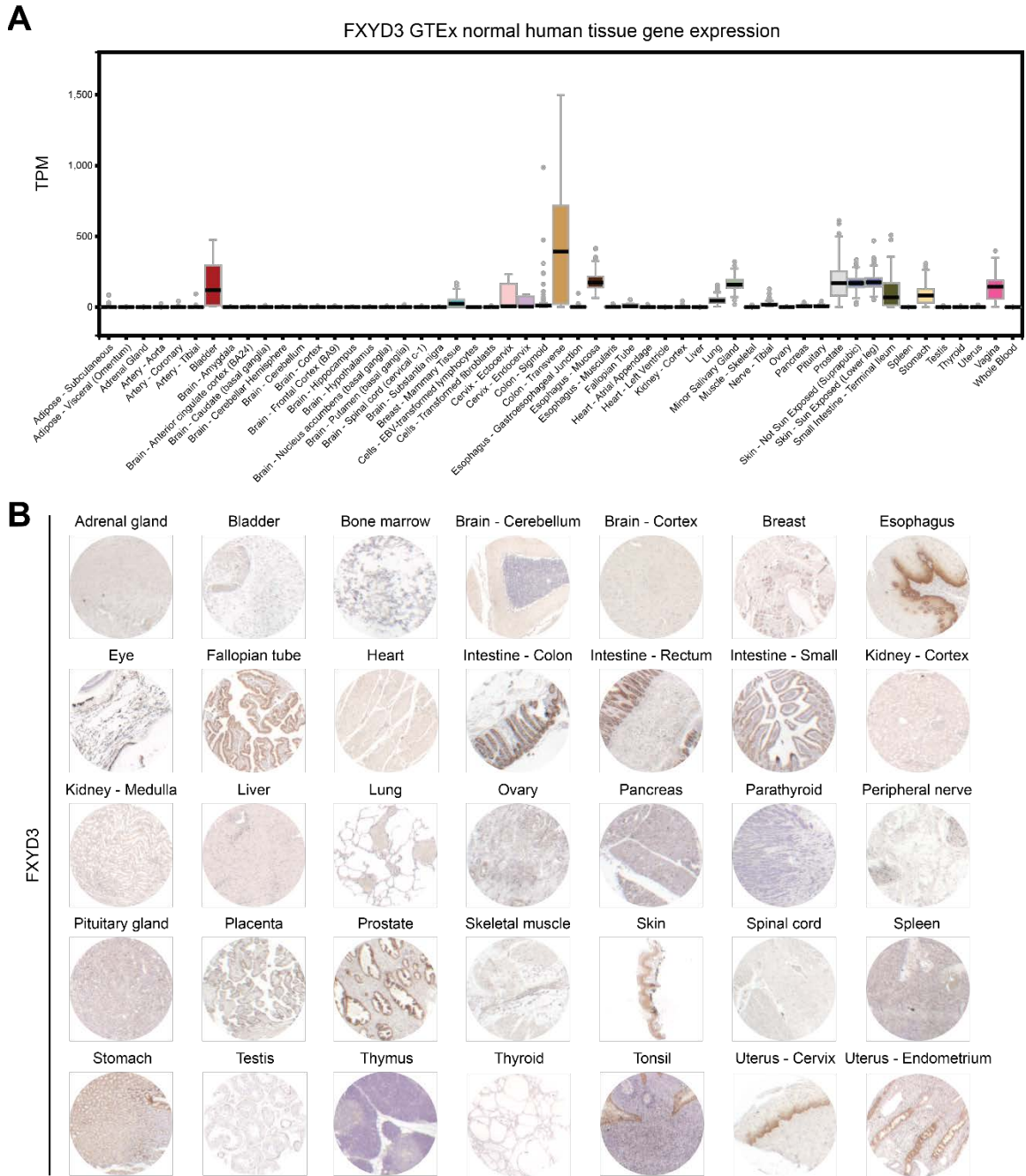


Fig. S5. Survey of the systemic expression of FXYD3 in normal human tissues. (A) Plot of FXYD3 gene expression across a variety of normal human tissues (in TPM or transcripts per million) from the NIH GTEx database via GTEx Portal. (B) FXYD3 immunohistochemical stains of a tissue microarray with 35 normal human tissues represented.

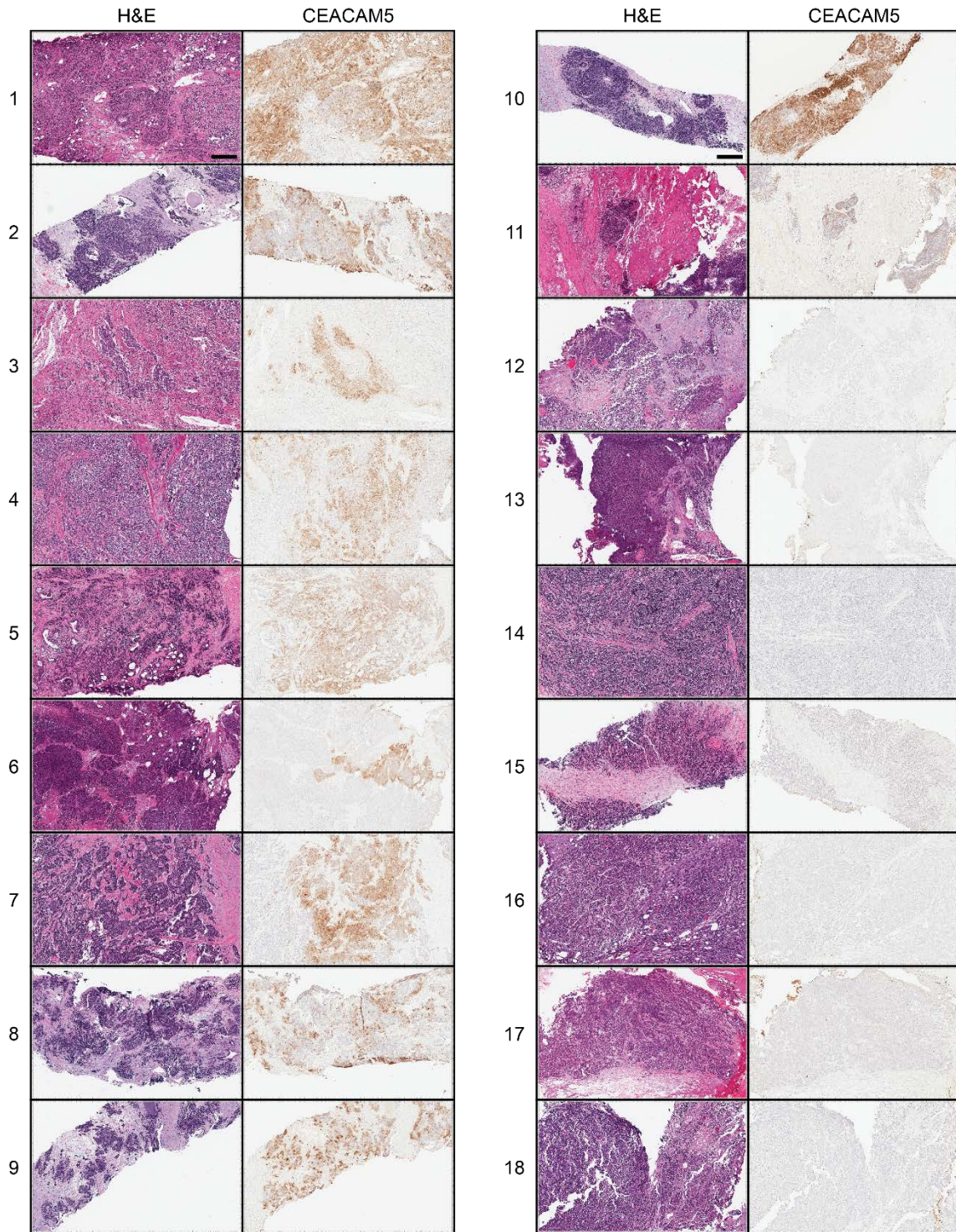


Fig. S6. Evaluation of CEACAM5 expression in a series of small cell NEPC cases. H&E and CEACAM5 immunohistochemical stains of 18 independent small cell NEPC samples archived at UCLA. Scale bar represents 200 μ m.

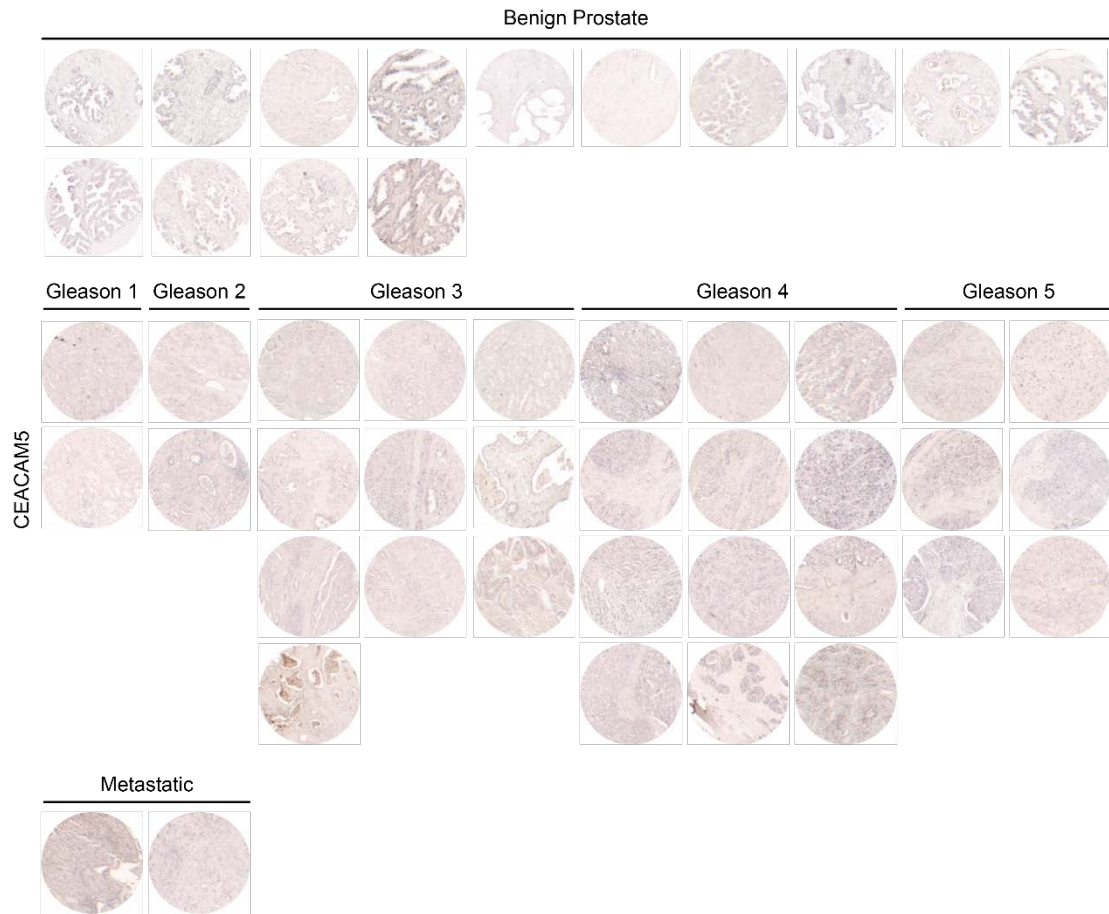


Fig. S7. Evaluation of CEACAM5 expression in a prostate cancer progression tissue microarray. CEACAM5 immunohistochemical stains of benign prostate tissues (n=14), primary Gleason grade 1-5 PrAd tissues (n=32), and metastatic PrAd samples (n=2).

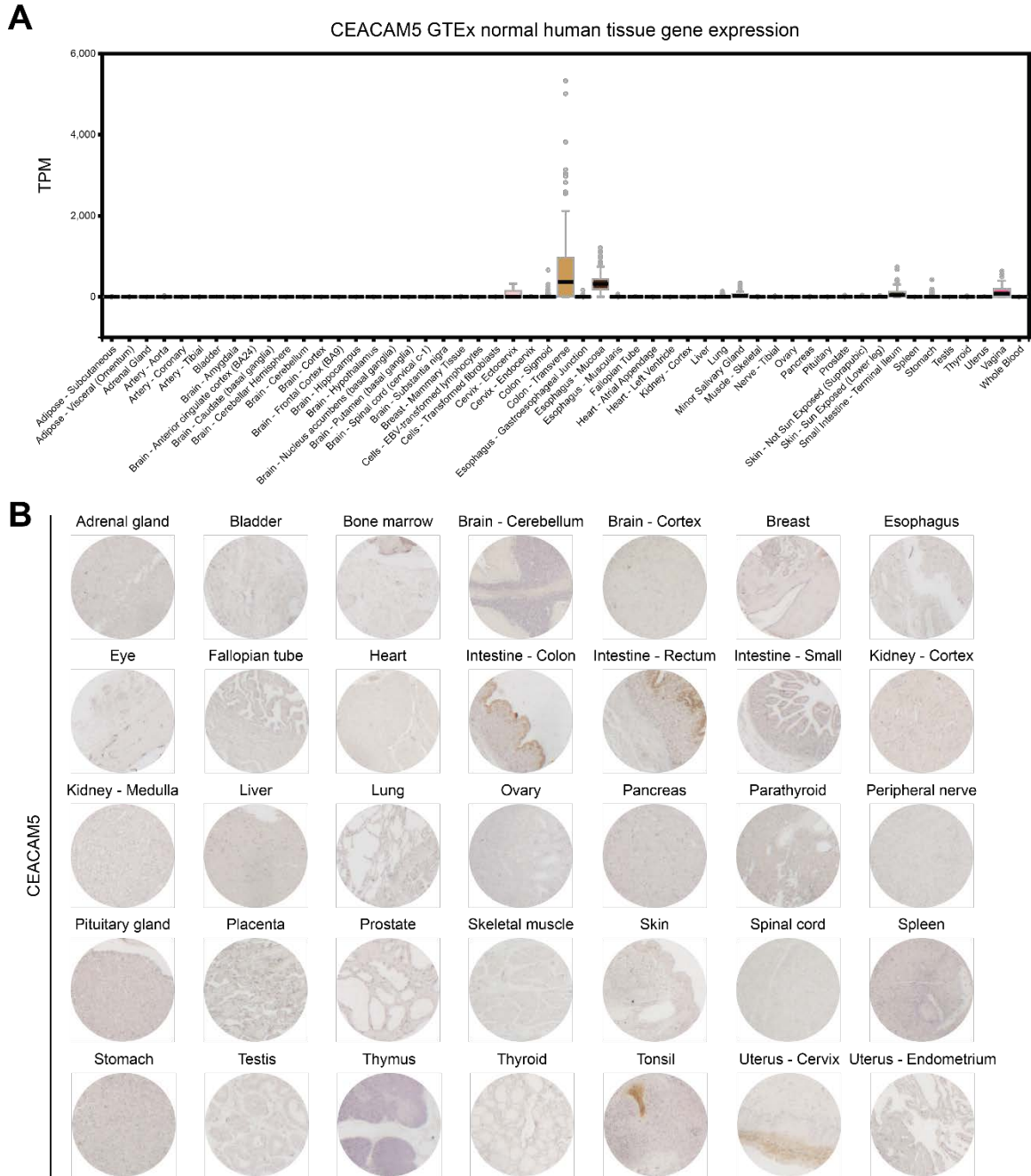


Fig. S8. Survey of the systemic expression of CEACAM5 in normal human tissues. (A) Plot of CEACAM5 gene expression across a variety of normal human tissues (in TPM or transcripts per million) from the NIH GTEx database via GTEx Portal. (B) CEACAM5 immunohistochemical stains of a tissue microarray with 35 normal human tissues represented.

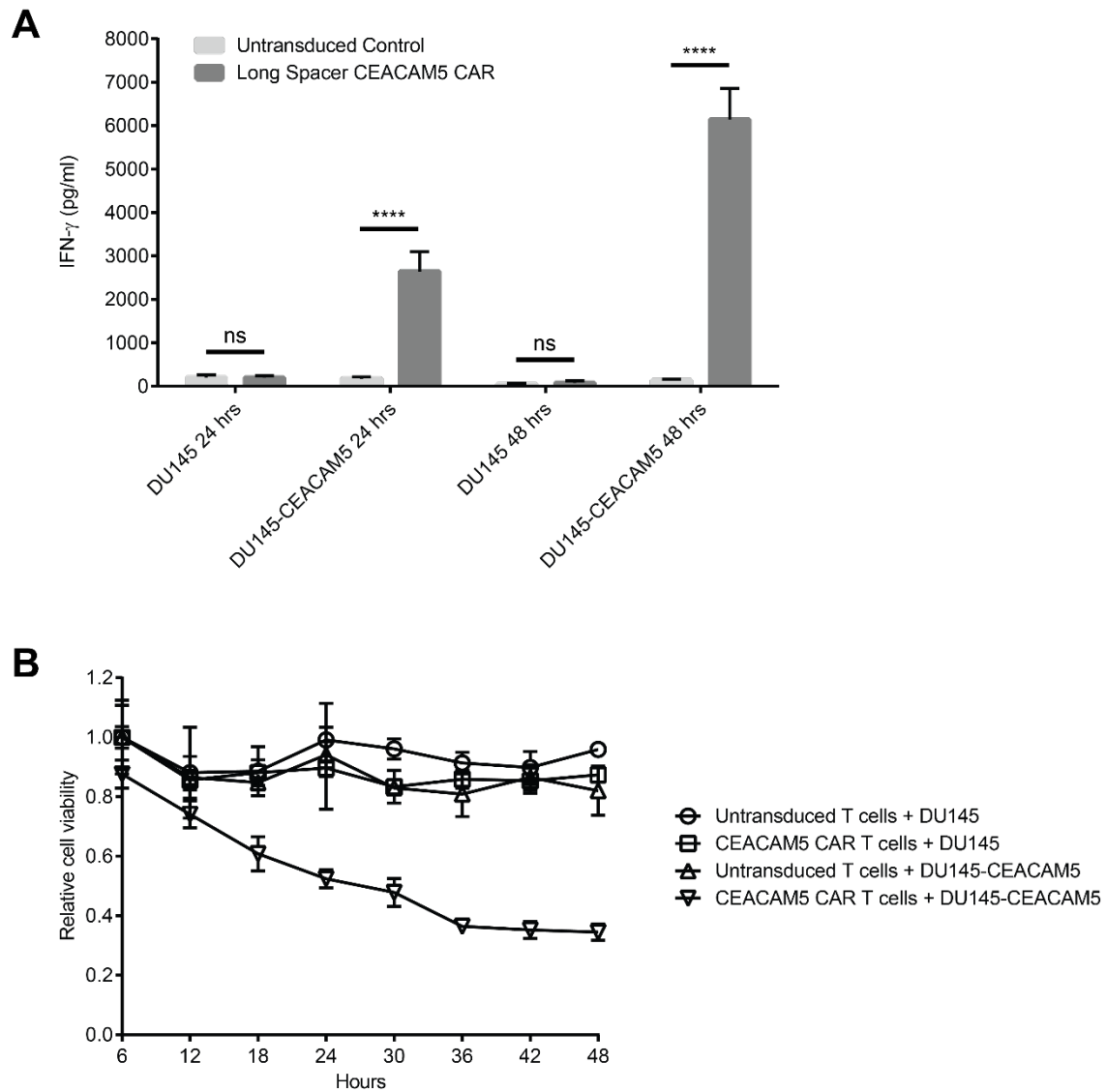


Fig. S9. Specificity of the cytotoxic activity of CEACAM5 CAR T cells in an engineered CEACAM5-positive prostate cancer cell line. (A) Interferon- γ (IFN- γ) quantitation in the media at 24 and 48 hours after co-culture of long spacer CEACAM5 CAR-transduced or untransduced T cells with CEACAM5-negative DU145 target cells or CEACAM5-positive DU145-CEACAM5 target cell lines at a 1:1 effector-to-target ratio. Standard error measurements for 3 replicate wells are displayed. ns represents non-significance and **** represents $p < 0.0001$ by two-way ANOVA statistical analysis. (B) Relative viability over time of CEACAM5-negative DU145 target cells and engineered CEACAM5-positive DU145-CEACAM5 target cells co-cultured with long spacer CEACAM5 CAR-transduced T cells at a 1:1 effector-to-target ratio. Standard error measurements for 3 replicate wells at each timepoint are displayed.

References

1. Lee JK, *et al.* (2016) N-Myc Drives Neuroendocrine Prostate Cancer Initiated from Human Prostate Epithelial Cells. *Cancer cell* 29(4):536-547.
2. Gao D, *et al.* (2014) Organoid cultures derived from patients with advanced prostate cancer. *Cell* 159(1):176-187.
3. Xin L, Ide H, Kim Y, Dubey P, & Witte ON (2003) In vivo regeneration of murine prostate from dissociated cell populations of postnatal epithelia and urogenital sinus mesenchyme. *Proceedings of the National Academy of Sciences of the United States of America* 100 Suppl 1:11896-11903.